

## Importance of the proligand-promolecule model in stereochemistry. II. The stereoisogram approach to stereoisomeric features of prismane derivatives

Shinsaku Fujita

Received: 11 April 2012 / Accepted: 18 April 2012 / Published online: 1 May 2012  
© Springer Science+Business Media, LLC 2012

**Abstract** The stereoisogram approach (Fujita in J Org Chem 69:3158–3165, 2004; and in Tetrahedron 60:11629–11638, 2004) has been applied to comprehensive discussions on geometric aspects and stereoisomeric aspects of stereochemistry, where a prismane skeleton has been selected as a rigid skeleton for the underlying proligand-promolecule model. The existence of five types of stereoisograms (Types I–V) has been demonstrated by using prismane derivatives as illustrative examples in a consistent way with a general proof using the group theory (Fujita in MATCH Commun Math Comput Chem 54:39–52, 2005). After a *C/A*-convention for characterizing absolute configurations was proposed on the basis of the stereoisogram approach, such geometric and stereoisomeric aspects of stereochemistry as chirality, *RS*-stereogenicity, and sclerality have been discussed by putting emphasis on the independence between chirality and *RS*-stereogenicity, on extended features of pseudoasymmetry, and on the assignability of *A/C*-descriptors. By following a general rationalization (Fujita in Tetrahedron 62:691–705, 2006), prochirality, pro-*RS*-stereogenicity, and pro-sclerality have been discussed on the basis of such attributive terms as sphericities, *RS*-tropicitities, and cercalities, where illustrative examples are selected from prismane derivatives. Thereby, the stereoisogram approach has been clarified to be a versatile device for integrating geometric and stereoisomeric aspects of stereochemistry.

**Keywords** Prismane · Stereoisogram · Stereochemistry · Proligand · Promolecule · Prochirality · Pseudoasymmetry · *C/A*-descriptor

---

S. Fujita (✉)  
Shonan Institute of Chemoinformatics and Mathematical Chemistry, Kaneko 479-7, Ooimachi,  
Ashigara-Kami-Gun, Kanagawa 258-0019, Japan  
e-mail: shinsaku\_fujita@nifty.com

## 1 Introduction

Geometric aspects and stereoisomeric aspects are highly entangled in stereochemistry, so that there have emerged serious confusion to prevent comprehensive understandings. From the beginning of stereochemistry founded by van't Hoff [43,44] and Le Bel [42] during the 1870s, the term “asymmetry” has been used equivocally, i.e., in a geometric meaning and in a stereoisomeric meaning. The original connotation of “an asymmetric carbon atom” due to van't Hoff [43,44] means (H1) being chiral (optically active) in a geometric meaning as well as (H2) the presence of a pair of enantiomers in a stereoisomeric meaning. The items H1 and H2 have been usually regarded as stating the same thing by different words, because the presence of stereoisomers (enantiomers) of the item H2 results in chirality of item H1.

After Fischer discovered sugar derivatives of exceptional cases to asymmetry [3–5], however, the term “pseudoasymmetry” was coined to characterize such exceptional cases. The term “pseudoasymmetry” has also been used equivocally i.e., in a geometric meaning and in a stereoisomeric meaning. Thus, the connotation of a pseudoasymmetric carbon atom means (F1) being achiral (optically inactive) in a geometric meaning as well as (F2) the presence of a pair of diastereomers in a stereoisomeric meaning. As exceptional cases, the item F2 has been mainly referred to in the conventional stereochemistry, so that the item F1 has been put little stress as a matter of course. Note that the presence of stereoisomers (diastereomers) of the item F2 does not result in chirality but in achirality of F1.

In spite of enormous efforts, the conventional stereochemistry have not reached a rational understandings on the differentiation between “asymmetry” (H1/H2) and “pseudoasymmetry” (F1/F2), where the expression “rational understandings” means a logical understanding based on mathematics, but not a descriptive or intuitive understanding. In other word, the problems of the conventional “chirality” and stereogenicity”, of the conventional “prochirality” and “prostereogenicity”, of the conventional dichotomy between enantiomers and “diastereomers”, of the conventional dichotomy between enantiotopic relationships and “diastereotopic” ones, and of the transmuted term “enantiotopic” still remain, as pointed out in the subsection titles of a review by Fujita [6].

In order to comprehend stereochemistry, geometric aspects such as the items H1 and F1 and stereoisomeric aspects such as the items H2 and F2 should be discussed analytically and afterward integrated on a rational basis. A seemingly inseparable relationship between the items H1 and H2 or between the items F1 and F2 stems from the methodology of stereochemistry, in which two-dimensional (2D) structures (graphs) are extended into three-dimensional (3D) structures (the 2D-3D extension). In the accompanying paper, we have discussed the geometric aspects (H1 and F1) from a viewpoint of the 2D-3D extension. At that time, we have emphasized the importance of the proligand-promolecule model [7–9] in order to avoid the problem of the 2D-3D extension in the discussions on the geometric aspects (H1 and F1).

As a continuation, stereoisomeric aspects such as the items H2 and F2 should be discussed in harmony with the above-described geometric aspects, where the effect of the 2D–3D extension on the stereoisomeric aspects should be analyzed also on the basis the proligand-promolecule model. For the purpose of harmonizing geomet-

ric and stereoisomeric aspects, the concepts of *holantimers* and *stereoisograms* have been proposed by Fujita [10–12], where the proligand-promolecule model serves as its theoretical basis, as found in the footnote 22 and Subsection 3.4.1 of [10] and Section 3.1 of [12]. In order to discuss such stereoisomeric aspects as concerned with *RS*-descriptors, *pro-R/pro-S*-descriptors, and *E/Z*-descriptors, the stereoisogram approach was exemplified by compounds of ligancy 4, e.g., a tetrahedral skeleton [10–12], an allene skeleton [13–15], an ethylene skeleton [16], and a square planar skeleton [17].

The concepts of holantimers and stereoisograms, however, can be applied to any rigid skeletons, because the proligand-promolecule model underlies these concepts. This feature of the stereoisogram approach has already been discussed by using an 8-methyl-8-azabicyclo[3.2.1]octane skeleton as a bicyclic skeleton in an original formulation [12] as well as a cyclobutane skeleton as a monocyclic skeleton in a more sophisticated formulation [18]. The availability of any rigid skeletons in the stereoisogram approach has been also described by giving a general collection of five types [12] as well as by proving the existence of five types of stereoisograms generally for a skeleton of *G*-symmetry with *n*-positions [19].

The stereoisogram approach has brought about the proposal of *pro-RS*-stereogenicity in place of “prochirality” [20–22], the specification of chirality and *RS*-stereogenicity [23,24], and the proposal of a new scheme for investigating geometric and stereoisomeric features in stereochemistry [25]. As a more sophisticated device, correlation diagrams of stereoisograms have been proposed by Fujita [26,27]. This proposal has resulted in the theory of organic stereoisogram in harmony with molecular symmetry [28], where a cyclobutane skeleton has been used as a skeleton of the proligand-promolecule model.

In the present series, we discuss geometrical and stereoisomeric aspects of stereochemistry by using a prismane skeleton as an additional example of a polycyclic skeleton for the proligand-promolecule model. In particular, we focus our attention on geometrical prochirality and extended pseudoasymmetry, which will provide us with more pieces of information than those given by the conventional concepts “prochirality” and “pseudoasymmetry”. For the purpose of succinct discussions, we emphasize the underlying proligand-promolecule model supporting both the USCI approach (Part I of this series) and the stereoisogram approach (Part II). This paper as Part II of this series deals with the stereoisogram approach based on the proligand-promolecule model.

## 2 Groups for characterizing prismane derivatives

### 2.1 *RS*-stereoisomeric group for a prismane skeleton

Let us number the six substitution sites (vertices) of a prismane skeleton sequentially to give a numbered skeleton **1** (Fig. 1), which is here called a *reference skeleton*. The initial mode of numbering shown by **1** is selected arbitrarily from  $6!$  (= 720) modes of numbering, because the selection of any numbering does not lose generality.

The prismane skeleton **1** belongs to the point group  $D_{3h}$  of order 12:

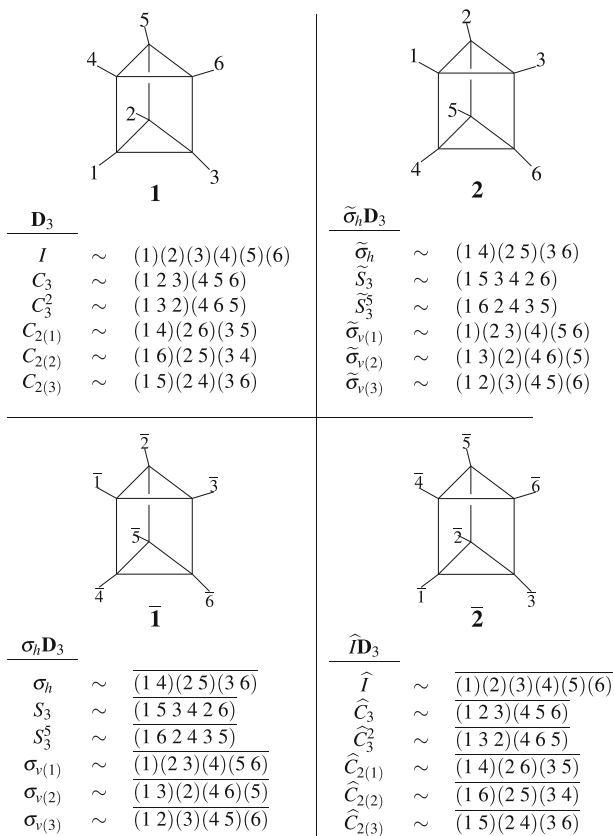


**Fig. 1** *RS*-stereoisomeric group  $\mathbf{D}_{3h\tilde{\sigma}_h\hat{I}} (= \mathbf{D}_{3h} + \tilde{\sigma}_h \mathbf{D}_{3h})$ , which is derived from coset representations  $\mathbf{D}_{3h}(/C_s)$

$$\mathbf{D}_{3h} = \{I, C_3, C_3^2, C_{2(1)}, C_{2(1)}, C_{2(3)}; \sigma_h, S_3, i, S_3^5, \sigma_{v(1)}, \sigma_{v(2)}, \sigma_{v(3)}\}. \tag{1}$$

By following Fujita’s USCI (unit-subduced-cycle-index) approach [29], the six substitution sites construct a six-membered orbit (equivalence class) governed by a coset representation  $\mathbf{D}_{3h}(/C_s)$  of degree 6 ( $= |\mathbf{D}_{3h}|/|C_{3v}| = 12/6$ ), as discussed in Part I of this series. The concrete permutations of the coset representation  $\mathbf{D}_{3h}(/C_s)$  are collected in the left part of Fig. 1 in the form of products of cycles, where an overbar indicates the alternation of the absolute configuration of each proligand. The notation with an overbar has been originated [30–33] for the purpose of emphasizing such alternation of ligand configurations as based on the proligand-promolecule model [7,29]. For a discussion on coset representations and a mark table of  $\mathbf{D}_{3h}$ , see Ref. [34,35].

Among the 12 elements, six proper rotations (chiral elements) construct the following subgroup  $\mathbf{D}_3$ :

$$\mathbf{D}_3 = \{I, C_3, C_3^2, C_{2(1)}, C_{2(1)}, C_{2(3)}\}, \tag{2}$$

which is the maximum chiral subgroup of  $\mathbf{D}_{3h}$ . The action of each element of  $\mathbf{D}_3$  (Eq. 2) on the skeleton  $\mathbf{1}$  generates a skeleton with homomeric numbering, which is regarded as being equivalent to the original skeleton  $\mathbf{1}$ .

The point group  $\mathbf{D}_{3h}$  is composed of two cosets concerned with its subgroup  $\mathbf{D}_3$  so as to be represented by the following coset decomposition:

$$\mathbf{D}_{3h} = \mathbf{D}_3 + \sigma_h \mathbf{D}_3, \quad (3)$$

Note that the product of cycles for the coset  $\sigma_h \mathbf{D}_3$  (i.e., reflections) has an overbar, which indicates the alternation of chirality senses of proligands (reflection of ligand chirality). As a result, the elements of the coset  $\sigma_h \mathbf{D}_3$  (i.e., rotoreflections) convert the reference skeleton  $\mathbf{1}$  into skeletons with homomeric modes of numbering, which are equivalent to another reference skeleton  $\bar{\mathbf{1}}$  under the action of  $\mathbf{D}_3$  (Eq. 2). Note that the skeleton  $\bar{\mathbf{1}}$  corresponds to the element  $\sigma_h$  ( $\sim (\bar{1} \ 4)(2 \ 5)(3 \ 6)$ ), which is contained in the coset  $\sigma_h \mathbf{D}_3$ .

Following the stereoisogram approach [10, 12], suppose that the symbol  $\tilde{\sigma}_h$  denotes the same permutation as  $\sigma_h$  but with no alternation of ligand configurations and that the symbol  $\hat{I}$  denotes the same permutation as the identity element  $I$  but with the alternation of ligand chirality senses. Thereby, there appear two additional groups derived from  $\mathbf{D}_3$  as follows:

$$\mathbf{D}_{3\tilde{\sigma}} = \mathbf{D}_3 + \tilde{\sigma}_h \mathbf{D}_3 \quad (4)$$

$$\mathbf{D}_{3\hat{I}} = \mathbf{D}_3 + \hat{I} \mathbf{D}_3, \quad (5)$$

where the group  $\mathbf{D}_{3\tilde{\sigma}}$  is called an *RS-permutation group* (or an *RS-diastereomeric group*) and the group  $\mathbf{D}_{3\hat{I}}$  is called a *ligand-reflection group* (or a *holantimeric group*). By starting from the coset representation  $\mathbf{D}_{3h}(/C_s)$  collected in the left part of Fig. 1, the elements of the coset  $\tilde{\sigma}_h \mathbf{D}_3$  (Eq. 4) and those of the coset  $\hat{I} \mathbf{D}_3$  (Eq. 5) are correlated to products of cycles, as collected in the right part of Fig. 1.

By following the formulation by Fujita [11, 17, 36], the resulting cosets,  $\mathbf{D}_3$  (Eqs. 3–5),  $\sigma_h \mathbf{D}$  (Eq. 3),  $\tilde{\sigma}_h \mathbf{D}_3$  (Eq. 4), and  $\hat{I} \mathbf{D}_3$  (Eq. 5) are collected to give an *RS-stereoisomeric group*:

$$\mathbf{D}_{3h\tilde{\sigma}\hat{I}} = \mathbf{D}_3 + \sigma_h \mathbf{D}_3 + \tilde{\sigma}_h \mathbf{D}_3 + \hat{I} \mathbf{D}_3, \quad (6)$$

whose concrete elements and the corresponding products of cycles are shown in Fig. 1. This equation represents a coset decomposition of the resulting *RS-stereoisomeric group*  $\mathbf{D}_{3h\tilde{\sigma}\hat{I}}$  by the subgroup  $\mathbf{D}_3$ , which contains rotations (proper rotations) only (Eq. 2). The following coset decompositions should be mentioned:

$$\mathbf{D}_{3h\tilde{\sigma}\hat{I}} = \mathbf{D}_{3h} + \tilde{\sigma}_h \mathbf{D}_{3h} = \mathbf{D}_{3h} + \hat{I} \mathbf{D}_{3h} \quad (7)$$

$$= \mathbf{D}_{3\tilde{\sigma}} + \hat{I} \mathbf{D}_{3\tilde{\sigma}} = \mathbf{D}_{3\tilde{\sigma}} + \sigma_h \mathbf{D}_{3\tilde{\sigma}} \quad (8)$$

$$= \mathbf{D}_{3\hat{I}} + \sigma_h \mathbf{D}_{3\hat{I}} = \mathbf{D}_{3\hat{I}} + \tilde{\sigma}_h \mathbf{D}_{3\hat{I}}, \quad (9)$$

which show the capability of selecting representatives.

The 24 permutations (products of cycles) listed in Fig. 1 construct a group of order 24, just as the 24 elements listed in Fig. 1 construct the *RS-stereoisomeric group*  $\mathbf{D}_{3h\tilde{\sigma}\hat{I}}$

of order 24. For the sake of simplicity, they are equalized tentatively in the present article because such a simplified treatment causes no confusion.

### 2.2 Quadruplet of reference skeletons

The action of the *RS*-stereoisomeric group  $\mathbf{D}_{3h\tilde{\sigma}\hat{I}}$  (order:  $|\mathbf{D}_{3h\tilde{\sigma}\hat{I}}| = 24$ ) on the skeleton **1** (Fig. 1) generates 24 *RS*-stereoisomeric skeletons, which are divided into four parts in accord with the coset decomposition represented by Eq. 6. Following the terminology of the stereoisogram approach [10, 12], the elements contained in the coset  $\mathbf{D}_3 (= I\mathbf{D}_3)$  in Fig. 1 are called *rotations*, the elements of the coset  $\sigma_h\mathbf{D}_3$  are called *rotoreflections*, the elements of the coset  $\tilde{\sigma}_h\mathbf{D}_3$  are called *RS-permutations*, and the elements of the coset  $\hat{I}\mathbf{D}_3$  are called *ligand reflections*.

Once the mode of reference numbering in **1** is assigned to the identity element *I* ( $= (1)(2)(3)(4)(5)$ ), the action of each element contained in the coset  $I\mathbf{D}_3 (= \mathbf{D}_3)$  produces a skeleton with a homomeric mode of numbering, which is regarded as being identical with the original skeleton **1**. This indicates that the skeleton **1** is a representative of six skeletons corresponding to the coset  $I\mathbf{D}_3 (= \mathbf{D}_3)$ .

On the same line, each element of the transversal listed in the right-hand side of Eq. 6, i.e., *I*,  $\sigma_h$ ,  $\tilde{\sigma}_h$ , or  $\hat{I}$ , corresponds to a prismane skeleton, **1**,  $\bar{\mathbf{1}}$ , **2**, or  $\bar{\mathbf{2}}$ , each of which is regarded as a representative of six reference skeletons assigned to the corresponding coset (Eq. 6), i.e.,  $\mathbf{D}_3$ ,  $\sigma_h\mathbf{D}_3$ ,  $\tilde{\sigma}_h\mathbf{D}_3$ , or  $\hat{I}\mathbf{D}_3$ , as collected in Fig. 1.

Because the subgroup  $\mathbf{D}_3$  of order 6 ( $|\mathbf{D}_3| = 6$ ), which is originally regarded as a point group, is a normal subgroup of the *RS*-stereoisomeric group  $\mathbf{D}_{3h\tilde{\sigma}\hat{I}}$  from the present viewpoint, the coset decomposition represented by Eq. 6 provides the following factor group of order 4:

$$\mathbf{D}_{3h\tilde{\sigma}\hat{I}}/\mathbf{D}_3 = \{\mathbf{D}_3, \sigma_h\mathbf{D}_3, \tilde{\sigma}_h\mathbf{D}_3, \hat{I}\mathbf{D}_3\}, \tag{10}$$

where the coset  $\mathbf{D}_3$  plays as an identity element. The transversal appearing in Eq. 10 constructs a group of order 4 as follows:

$$\text{Tv}(\mathbf{D}_{3h\tilde{\sigma}\hat{I}}/\mathbf{D}_3) = \{I, \sigma_h, \tilde{\sigma}_h, \hat{I}\}. \tag{11}$$

The multiplication table for the factor group  $\mathbf{D}_{3h\tilde{\sigma}\hat{I}}/\mathbf{D}_3$  (Eq. 10) and the corresponding table of the transversal group  $\text{Tv}(\mathbf{D}_{3h\tilde{\sigma}\hat{I}}/\mathbf{D}_3)$  (Eq. 11) are obtained as follows:

$\mathbf{D}_{3h\tilde{\sigma}\hat{I}}/\mathbf{D}_3$	$\mathbf{D}_3$	$\sigma_h\mathbf{D}_3$	$\tilde{\sigma}_h\mathbf{D}_3$	$\hat{I}\mathbf{D}_3$	$\text{Tv}(\mathbf{D}_{3h\tilde{\sigma}\hat{I}}/\mathbf{D}_3)$	<i>I</i>	$\sigma_h$	$\tilde{\sigma}_h$	$\hat{I}$
$\mathbf{D}_3$	$\mathbf{D}_3$	$\sigma_h\mathbf{D}_3$	$\tilde{\sigma}_h\mathbf{D}_3$	$\hat{I}\mathbf{D}_3$	<i>I</i>	<i>I</i>	$\sigma_h$	$\tilde{\sigma}_h$	$\hat{I}$
$\sigma_h\mathbf{D}_3$	$\sigma_h\mathbf{D}_3$	$\mathbf{D}_3$	$\hat{I}\mathbf{D}_3$	$\tilde{\sigma}_h\mathbf{D}_3$	$\sigma_h$	$\sigma_h$	<i>I</i>	$\hat{I}$	$\tilde{\sigma}_h$
$\tilde{\sigma}_h\mathbf{D}_3$	$\tilde{\sigma}_h\mathbf{D}_3$	$\hat{I}\mathbf{D}_3$	$\mathbf{D}_3$	$\sigma_h\mathbf{D}_3$	$\tilde{\sigma}_h$	$\tilde{\sigma}_h$	$\hat{I}$	<i>I</i>	$\sigma_h$
$\hat{I}\mathbf{D}_3$	$\hat{I}\mathbf{D}_3$	$\tilde{\sigma}_h\mathbf{D}_3$	$\sigma_h\mathbf{D}_3$	$\mathbf{D}_3$	$\hat{I}$	$\hat{I}$	$\tilde{\sigma}_h$	$\sigma_h$	<i>I</i>

(12)

The factor group  $\mathbf{D}_{3h\tilde{\sigma}\hat{I}}/\mathbf{D}_3$  (Eq. 10) is isomorphic to the Klein four-group as well as to the point group  $\mathbf{C}_{2v}$ . Because these groups have five subgroups only, we have

reached a general proof for the presence of five types of *RS*-stereoisomers (Types I–V) [19]:

$$\text{Type III} \leftrightarrow \{\mathbf{D}_3\}, \quad (13)$$

$$\text{Type II} \leftrightarrow \{\mathbf{D}_3, \tilde{\sigma}_h \mathbf{D}_3\}, \quad (14)$$

$$\text{Type I} \leftrightarrow \{\mathbf{D}_3, \widehat{\mathbf{I}}\mathbf{D}_3\}, \quad (15)$$

$$\text{Type V} \leftrightarrow \{\mathbf{D}_3, \sigma_h \mathbf{D}_3\}, \quad (16)$$

$$\text{Type IV} \leftrightarrow \{\mathbf{D}_3, \sigma_h \mathbf{D}_3, \tilde{\sigma}_h \mathbf{D}_3, \widehat{\mathbf{I}}\mathbf{D}_3\} \quad (17)$$

Note that the factor group  $\{\mathbf{D}_3\}$  for Type III corresponds to the maximum chiral subgroup  $\mathbf{D}_3$  (Eq. 2), the factor group  $\{\mathbf{D}_3, \tilde{\sigma}_h \mathbf{D}_3\}$  for Type II corresponds to the *RS*-permutation group  $\mathbf{D}_{3\tilde{\sigma}}$  (Eq. 4), the factor group  $\{\mathbf{D}_3, \widehat{\mathbf{I}}\mathbf{D}_3\}$  for Type I corresponds to the ligand-reflection group  $\mathbf{D}_{3\widehat{\mathbf{I}}}$  (Eq. 5), the factor group  $\{\mathbf{D}_3, \sigma_h \mathbf{D}_3\}$  for Type V corresponds to the point group  $\mathbf{D}_{3h}$  (Eq. 3), and the factor group  $\{\mathbf{D}_3, \sigma_h \mathbf{D}_3, \tilde{\sigma}_h \mathbf{D}_3, \widehat{\mathbf{I}}\mathbf{D}_3\}$  for Type IV corresponds to the *RS*-stereoisomeric group  $\mathbf{D}_{3h\tilde{\sigma}\widehat{\mathbf{I}}}$  (Eq. 6).

The categorization shown by Eqs. 13–17 holds true for any group  $\mathbf{G}_C$  given in place of  $\mathbf{D}_3$ , because any group  $\mathbf{G}_C$  is capable of constructing such an *RS*-stereoisomeric group (Eq. 6) so as to give the corresponding factor group of order 4 such as Eq. 10 [19]. The crux of the general proof [19] is the operation  $\widehat{\mathbf{I}}$  linked to the presence of holantimers, which has been first proposed by Fujita in the stereoisogram approach [10, 12].

The *RS*-stereoisomeric group  $\mathbf{D}_{3h\tilde{\sigma}\widehat{\mathbf{I}}}$  (Eq. 6) is concerned with a reference skeleton (e.g., **1**). It follows that each prismane derivative exhibits an appropriate subgroup of the *RS*-stereoisomeric group  $\mathbf{D}_{3h\tilde{\sigma}\widehat{\mathbf{I}}}$  (Eq. 6). Discussions on the basis of factor groups are also effective even to the latter subgroup. On the same line, such discussions on the basis of factor groups are effective even when degeneration occurs for a given skeleton (such as a square planar skeleton) [17].

### 2.3 Three attributes and three relationships for stereoisograms

According to the stereoisogram approach [10, 12], these four categories of elements collected in Fig. 1 (i.e., rotations, rotoreflections, *RS*-permutations, and ligand reflections) are operated to prismane derivatives as follows:

$$\text{rotations } (\in \mathbf{D}_3) : \quad \mathbf{1}, \bar{\mathbf{1}}, \mathbf{2}, \bar{\mathbf{2}} \text{ stabilized} \implies \text{homomeric} \quad (18)$$

$$\text{rotoreflections } (\in \sigma_h \mathbf{D}_3) : \quad \mathbf{1} \leftrightarrow \bar{\mathbf{1}} \text{ and } \mathbf{2} \leftrightarrow \bar{\mathbf{2}} \implies \text{enantiomeric} \quad (19)$$

$$\text{RS-permutations } (\in \tilde{\sigma}_h \mathbf{D}_3) : \quad \mathbf{1} \leftrightarrow \mathbf{2} \text{ and } \bar{\mathbf{1}} \leftrightarrow \bar{\mathbf{2}} \implies \text{RS-diastereomeric} \quad (20)$$

$$\text{ligand reflections } (\in \widehat{\mathbf{I}}\mathbf{D}_3) : \quad \mathbf{1} \leftrightarrow \bar{\mathbf{2}} \text{ and } \bar{\mathbf{1}} \leftrightarrow \mathbf{2} \implies \text{holantimeric}, \quad (21)$$

where there appear three types of pairwise relationships in addition of trivial homomeric relationships due to the rotations ( $\in \mathbf{D}_3$ ) which convert **1**,  $\bar{\mathbf{1}}$ , **2**, and  $\bar{\mathbf{2}}$  into themselves.

The three pairwise relationships in addition to the homomeric relationships (Eqs. 18–21) in combination with the factor group (Eq. 10) enable us to clarify the

**Table 1** Three relationships and the corresponding attributes appearing in stereoisograms [12]

symbol	relationship	attribute
(Concerned with reflections $\odot$ )		
$\leftarrow \bullet \rightarrow$	enantiomeric	chiral
$\equiv \bullet \equiv$	(self-enantiomeric)	achiral
(Concerned with <i>RS</i> -permutations $\circ$ )		
$\leftarrow \circ \rightarrow$	<i>RS</i> -diastereomeric	<i>RS</i> -stereogenic
$\equiv \circ \equiv$	(self- <i>RS</i> -diastereomeric)	<i>RS</i> -astereogenic
(Concerned with ligand reflections $\bullet$ )		
$\leftarrow \bullet \rightarrow$	holantimeric	scleral
$\equiv \bullet \equiv$	(self-holantimeric)	ascleral

stereochemical properties of the subgroups of the *RS*-stereoisomeric group, i.e., the point group  $D_{3h}$  (Eq. 1), the *RS*-permutation group  $D_{3\bar{\sigma}}$  (Eq. 4), and the ligand-reflection group  $D_{3\bar{\Gamma}}$  (Eq. 5). Thereby, such relationships as described above are integrated to give *RS*-stereoisomeric relationships, which are related to attributive terms such as chirality and *RS*-stereogenicity, as summarized in Table 1. The symbols and notations used in Table 1 are in accord with Ref. [12].

## 2.4 Construction of stereoisograms

In order to exemplify procedures of constructing stereoisograms [10–12], we first show a procedure of constructing a stereoisogram of prismane itself, which exhibits Type IV character with a full symmetry, i.e., the *RS*-stereoisomeric group  $D_{3h\bar{\sigma}\bar{\Gamma}}$  (Eq. 6).

Suppose that six hydrogen atoms (as achiral proligands) are placed on the six substitution sites (vertices) of the prismane skeleton **1** in terms of the following function:

$$f_1 : f_1(1) = f_1(2) = f_1(3) = f_1(4) = f_1(5) = f_1(6) = H \quad (22)$$

in accord with the proligand-promolecule model [7, 29]. In most cases so long as no confusion emerges, the terms *proligands* and *promolecules* of the proligand-promolecule model may be equalized to terms *ligands* and *molecules* for the sake of simplicity (cf. Chapter 21 of [29]). Thereby, the quadruplet of skeletons (**1**,  $\bar{\mathbf{1}}$ , **2**, and  $\bar{\mathbf{2}}$  shown in Fig. 1) generates promolecules (named *RS*-stereoisomers) of the same kind (**3**,  $\bar{\mathbf{3}}$ ,  $\mathbf{3}'$ , and  $\bar{\mathbf{3}}'$ ).

After the four promolecules of the quadruplet are aligned in a square planar fashion as depicted in Fig. 2, the three kinds of equality symbols with an open circle, a solid circle, and an encircled solid circle (Table 1) are added so as to construct a stereoisogram of Type IV. As a result, the quadruplet of promolecules (**3**,  $\bar{\mathbf{3}}$ ,  $\mathbf{3}'$ , and  $\bar{\mathbf{3}}'$ ) is degenerated into a single promolecule of  $D_{3h}$ -symmetry (**3**) so as to form the stereoisogram of Type IV (Fig. 2), which belongs to the *RS*-stereoisomeric group  $D_{3h\bar{\sigma}\bar{\Gamma}}$ .

As a second example, suppose that six achiral proligands (2H, 2A, and 2W) are placed on the six substitution sites (vertices) of the prismane skeleton **1** in accord with the function:



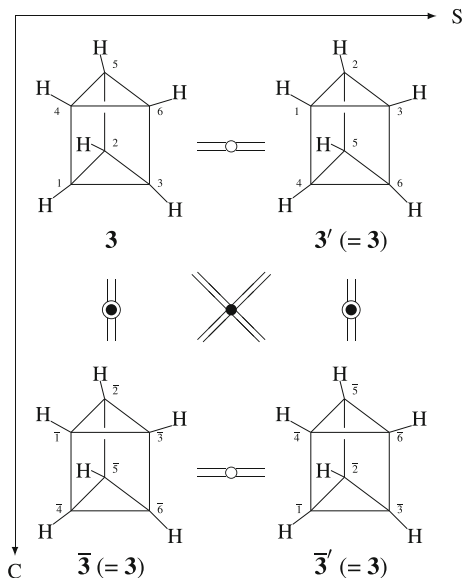


**Fig. 2** Stereoisogram of Type IV for prismane as a prismane skeleton with the constitution  $H_6$ , which exhibits the full symmetry of  $D_{3h}$ . The stereoisogram of Type IV belongs to the  $RS$ -stereoisomeric group  $D_{3h\bar{\sigma}\hat{T}}$

$$f_2 : f_2(1) = H, f_2(2) = W, f_2(3) = A, f_2(4) = H, f_2(5) = A, f_2(6) = W. \quad (23)$$

where the proligand-promolecule model [7, 29] is taken into consideration. Thereby, the quadruplet of skeletons (**1**, **1**, **2**, and **2** shown in Fig. 1) generates promolecules, i.e., **4**, **4** (= **5**), **5** (= **4**) and **5** (= **4**).

The stereoisogram of Type I (Fig. 3) for prismane derivatives with the constitution  $H_4A_2W_2$  is characterized by the presence of diagonal equality symbols according the stereoisogram approach [10, 12]. As a result, the four promolecules of the stereoisogram of Type I (Fig. 3) are regarded as two pairs of enantiomers **4/4** and **5/5** which are in an  $RS$ -diastereomeric relationship. Note that the  $RS$ -diastereomeric relationship between **4** and **5** (= **4**) is superposed onto the enantiomeric relationship between **4** and **4** (= **5**). The two relationship are equalized to be degenerated into a single enantiomeric relationship so that the  $RS$ -diastereomeric relationship is ignored in the conventional stereochemistry.

According to the stereoisogram approach [10, 12], the stereoisogram of Type I (Fig. 3) belongs to a ligand-reflection group  $C_{2\hat{T}}$ , which is represented as follows:

$$C_{2\hat{T}} = \{I, C_{2(1)}, \hat{T}, \hat{C}_{2(1)}\} \quad (24)$$

$$\sim \{(1)(2)(3)(4)(5)(6), (1\ 4)(2\ 6)(3\ 5), \\ \overline{(1)(2)(3)(4)(5)(6)}, \overline{(1\ 4)(2\ 6)(3\ 5)}\}. \quad (25)$$

The group  $C_{2\hat{T}}$  (Eq. 25) is a subgroup of the ligand-reflection group  $D_{3\hat{T}}$  ( $\subset D_{3h\bar{\sigma}\hat{T}}$ ). See Eqs. 5 and 15.

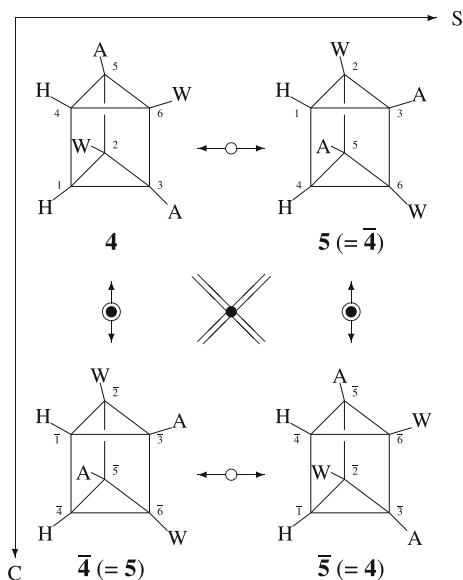


**Fig. 3** Stereoisogram of Type I for prismane derivatives with the constitution  $H_4A_2W_2$ , which exhibits the symmetry of  $C_2$ . The stereoisogram of Type I belongs to the ligand-reflection group  $C_{2\hat{T}}$ , which is a subgroup of  $D_{3\hat{T}} (C D_{3h\hat{T}})$

### 2.5 Five types of stereoisograms for prismane derivatives

According to the stereoisogram approach [10, 12], stereoisograms of five types are drawn by starting from a prismane skeleton, as collected in Fig. 4. Although the collection of stereoisograms in Fig. 4 is drawn by using appropriate sets of proligands as representatives, it is consistent to a general diagram reported in Fig. 6 of [12]. The collection shown in Fig. 4 is divided into four parts with double lines by considering chirality/achirality (along the vertical chirality(C)-axis) and *RS*-stereogenicity/*RS*-astereogenicity (along the horizontal *RS*-stereogenicity(S)-axis). The diagonal directions of each stereoisogram are concerned with scleral/ascleral properties, which provide us with the definition of holantimers [10, 12].

The Type I stereoisogram of Fig. 4 is concerned with a pair of enantiomeric prismane derivatives  $\underline{6}/\overline{6}$  with the constitution  $H_2A_2p\overline{p}$  (or the partition [2,2,0,0,0,0;1,1,0,0] according to Part I of this series). In terms of point groups,  $\underline{6}$  (or  $\overline{6}$ ) belongs to  $C_1$ . Because the promolecule  $\underline{6}$  is fixed (stabilized) by a ligand reflection  $\widehat{C}_{2(1)}$  ( $= (1\ 4)(2\ 6)(3\ 5)$ ), the promolecule  $\underline{6}$  belongs to a ligand-reflection group represented as follows:

$$C_{\widehat{2}} = \{I, \widehat{C}_{2(1)}\} \tag{26}$$

$$\sim \{(1)(2)(3)(4)(5)(6), \overline{(1\ 4)(2\ 6)(3\ 5)}\}, \tag{27}$$

which is a subgroup of the ligand-reflection group  $D_{3\hat{T}}$  (Eq. 5). See also Eq. 15 for Type I. The resulting promolecule (identical with  $\underline{6}$ ) is homomeric to the promolecule  $\overline{7} (= \underline{6})$ ,

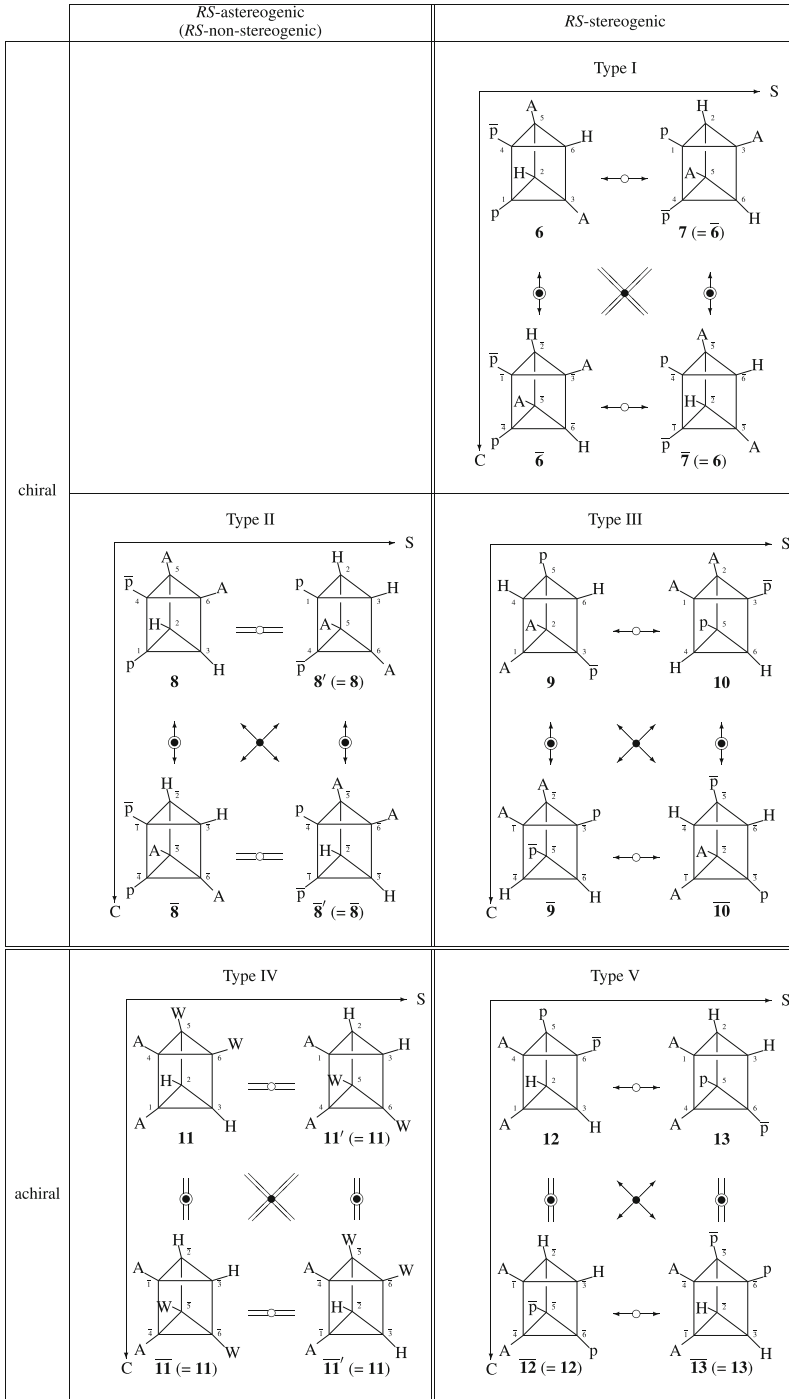


**Fig. 4** Stereoisograms of five types based on a prismane skeleton. The symbols H, A, and W denote achiral proligands in isolation, while a pair of symbols  $p$  and  $\bar{p}$  denotes a pair of enantiomeric proligands in isolation

which is obtained by the action of another ligand reflection  $\widehat{T} = \overline{(1)(2)(3)(4)(5)(6)}$ . The homomeric relationship between  $\widehat{6}$  and  $\overline{7} (= \widehat{6})$  is confirmed by the action of  $\mathbf{D}_3$ -group. Note that  $\widehat{C}_{2(1)} \in \widehat{T}\mathbf{D}_3$  and  $\widehat{T} \in \widehat{T}\mathbf{D}_3$ .

The Type II stereoisogram of Fig. 4 is concerned with another pair of enantiomeric prismane derivatives  $\mathbf{8}/\overline{\mathbf{8}}$  with the constitution  $\text{H}_2\text{A}_2\text{p}\overline{\text{p}}$  (or the partition  $[2,2,0,0,0,0;1,1,0,0]$  according to Part I of this series). As for a point group,  $\mathbf{8}$  (or  $\overline{\mathbf{8}}$ ) belongs to  $\mathbf{C}_1$ . Because the promolecule  $\mathbf{8}$  is fixed (stabilized) by an  $RS$ -permutation  $\widetilde{\sigma}_{v(1)} (= (1)(2\ 3)(4)(5\ 6))$ , the promolecule  $\mathbf{8}$  (or the corresponding stereoisogram) belongs to an  $RS$ -permutation group represented as follows:

$$\mathbf{C}_{1\widetilde{\sigma}} = \{I, \widetilde{\sigma}_{v(1)}\} \quad (28)$$

$$\sim \{(1)(2)(3)(4)(5)(6), (1)(2\ 3)(4)(5\ 6)\}, \quad (29)$$

which is a subgroup of the  $RS$ -permutation group  $\mathbf{D}_{3\widetilde{\sigma}}$  (Eq. 4). See also Eq. 14 for Type II. The resulting promolecule (identical with  $\mathbf{8}$ ) is homomeric to the promolecule  $\overline{\mathbf{8}}' (= \mathbf{8})$ , which is obtained by the action of another  $RS$ -permutation  $\widetilde{\sigma}_h (= (1\ 4)(2\ 5)(3\ 6))$ . The homomeric relationship between  $\mathbf{8}$  and  $\overline{\mathbf{8}}' (= \mathbf{8})$  is confirmed by the action of  $\mathbf{D}_3$ -group. Note that  $\widetilde{\sigma}_{v(1)} \in \widetilde{\sigma}_h\mathbf{D}_3$  and  $\widetilde{\sigma}_h \in \widetilde{\sigma}_h\mathbf{D}_3$ .

The Type III stereoisogram of Fig. 4 is concerned with two pairs of enantiomeric prismane derivatives  $\mathbf{9}/\overline{\mathbf{9}}$  and  $\mathbf{10}/\overline{\mathbf{10}}$ , both of which have the constitution  $\text{H}_2\text{A}_2\text{p}\overline{\text{p}}$  (or the partition  $[2,2,0,0,0,0;1,1,0,0]$  according to Part I of this series). As for a point group,  $\mathbf{9}$  (or  $\overline{\mathbf{9}}$ ) belongs to  $\mathbf{C}_1$ . Because the promolecule  $\mathbf{9}$  (or  $\mathbf{10}$ ) is fixed (stabilized) only by the identity element  $I (= (1)(2)(3)(4)(5)(6))$ , the promolecule  $\mathbf{9}$  belongs to the identity group  $\mathbf{C}_1$ , which is a subgroup of the point group  $\mathbf{D}_3$  (Eq. 2). See also Eq. 13 for Type III.

The Type IV stereoisogram of Fig. 4 is concerned with a single promolecule  $\mathbf{11}$  with the constitution  $\text{H}_2\text{A}_2\text{W}_2$  (or the partition  $[2,2,2,0,0,0;0,0,0,0]$  according to Part I of this series). As for a point group, the promolecule  $\mathbf{11}$  belongs to the point group  $\mathbf{C}_s$ . From the viewpoint of the stereoisogram approach, the promolecule  $\mathbf{11}$  belongs to an  $RS$ -stereoisomeric group represented as follows:

$$\mathbf{C}_{1\sigma\widehat{T}} = \{I, \sigma_{v(1)}, \widetilde{\sigma}_{v(1)}, \widehat{T}\} \quad (30)$$

$$\sim \{(1)(2)(3)(4)(5)(6), (1)(2\ 3)(4)(5\ 6), \\ \overline{(1)(2\ 3)(4)(5\ 6)}, \overline{(1)(2)(3)(4)(5)(6)}\}, \quad (31)$$

which is a subgroup of the  $RS$ -stereoisomeric group  $\mathbf{D}_{3h\sigma\widehat{T}}$  (Eq. 6). See also Eq. 17 for Type IV. It should be noted that the four promolecules appearing in the Type IV stereoisogram of Fig. 4 are depicted in accord with the group represented by Eq. 11. They are homomeric to the promolecules depicted by means of Eq. 31, which are identical to each other even without the action of  $\mathbf{D}_3$ . Each of the homomeric relationships (concerned with Eq. 11 vs. Eq. 31) is confirmed by the action of  $\mathbf{D}_3$ -group.

The Type V stereoisogram of Fig. 4 involves achiral promolecules  $\mathbf{12}$  and  $\mathbf{13}$  having the constitution  $\text{H}_2\text{A}_2\text{p}\overline{\text{p}}$  (or the partition  $[2,2,0,0,0,0;1,1,0,0]$  according to Part I of this series), which are in an  $RS$ -diastereomeric relationship. Geometrically speaking, they belong to the point group  $\mathbf{C}_s$ . Because the promolecule  $\mathbf{12}$  (or  $\mathbf{13}$ ) is fixed (sta-

bilized) by a reflection  $\sigma_{v(1)}$  ( $= \overline{(1)(2\ 3)(4)(5\ 6)}$ ), the promolecule **12** (or **13**) belong to a point group  $C_s$ :

$$C_s = \{I, \sigma_{v(1)}\} \quad (32)$$

$$\sim \{(1)(2)(3)(4)(5)(6), \overline{(1)(2\ 3)(4)(5\ 6)}\}, \quad (33)$$

which is a subgroup of the point group  $D_{3h}$  (Eq. 1). See also Eq. 16 for Type V.

The promolecule generated by  $C_s$  is identical with **12** (or **13**) and homomeric to the promolecule  $\overline{\mathbf{12}}$  ( $= \mathbf{12}$ ) or  $\overline{\mathbf{13}}$  ( $= \mathbf{13}$ ), which is obtained by the action of  $C'_s$  ( $= \{I, \sigma_h\}$ ). The homomeric relationship between **12** and  $\overline{\mathbf{12}}$  ( $= \mathbf{12}$ ) or between **13** and  $\overline{\mathbf{13}}$  ( $= \mathbf{13}$ ) is confirmed by the action of  $D_3$ -group. Note that  $\sigma_{v(1)} \in \sigma_h D_3$  and  $\sigma_h \in \sigma_h D_3$ .

### 3 Illustrative examples of stereoisograms for prismane derivatives

#### 3.1 Prismane derivatives with one achiral or chiral substituent

The symmetry-itemized combinatorial enumeration reported in Part I of this series (the [5,1,0,0,0,0;0,0,0,0]-row of Table 1 of Part 1) shows that there is one  $C_s$ -derivative having the constitution of  $H_5A$ . The corresponding stereoisogram exhibits Type IV properties, as shown in Fig. 5. Hereafter, we obey a convention of organic chemistry in which substitution of hydrogen atoms are implicit, not to be written in structural formulas. The stereoisogram of Type IV shown in Fig. 5 belongs to the  $RS$ -stereoisomeric group  $C_{1\sigma\hat{\sigma}\hat{\Gamma}}$  (Eq. 31), which is a subgroup of the  $RS$ -stereoisomeric group  $D_{3h\hat{\sigma}\hat{\Gamma}}$  (Eq. 6). See Eq. 17.

The value 1/2 at the intersection between the [5,0,0,0,0,0;1,0,0,0]-row and the  $C_1$  column in Table 1 of Part 1 indicates that there is one pair of  $C_1$ -derivatives ( $\mathbf{15}/\overline{\mathbf{15}}$ ) having the constitution of  $H_5p$  and  $H_5\bar{p}$ . Note that the value 1/2 corresponds to the term  $1 \times \frac{1}{2}(H_5p + H_5\bar{p})$  because a pair of enantiomers is counted once. The corresponding stereoisogram exhibits Type II properties, as shown in Fig. 6. The stereoisogram (Fig. 6) belongs to the  $RS$ -permutation group  $C_{1\hat{\sigma}}$  (Eq. 29), which is a subgroup of the  $RS$ -permutation group  $D_{3\hat{\sigma}}$  (Eq. 4). See Eq. 14. The  $RS$ -permutation group  $D_{3\hat{\sigma}}$  (Eq. 4) is in turn a subgroup of the  $RS$ -stereoisomeric group  $D_{3h\hat{\sigma}\hat{\Gamma}}$  (Eq. 6).

#### 3.2 Prismane derivatives with two achiral substituents

The [4,2,0,0,0,0;0,0,0,0]-row of Table 1 of Part 1 indicates that there are one pair of enantiomeric  $C_2$ -derivatives, one  $C_s$ -derivative, one  $C_{2v}$ -derivative, which have the constitution of  $H_4A_2$ .

The pair of enantiomeric  $C_2$ -derivatives ( $\mathbf{16}/\overline{\mathbf{16}}$ ) corresponds to a quadruplet of  $RS$ -stereoisomers which gives a stereoisogram of Type I, as shown in Fig. 7. Compare this with the stereoisogram of Type I shown in Fig. 3. The stereoisogram of Type I (Fig. 7) belongs to the ligand-reflection group  $C_{2\hat{\Gamma}}$  (Eq. 25), which is a subgroup of  $D_{3\hat{\Gamma}} \subset D_{3h\hat{\sigma}\hat{\Gamma}}$ . For the Type I character, see Eq. 15.

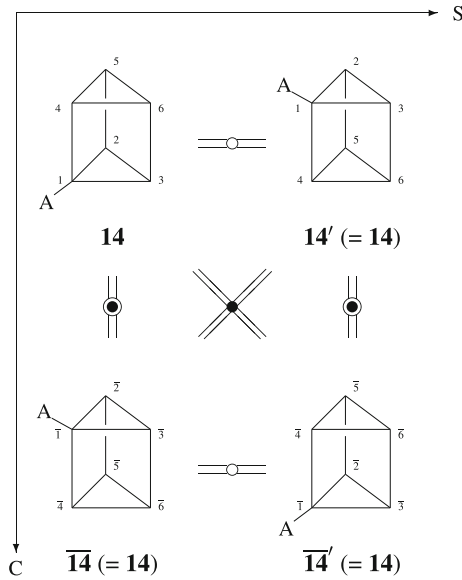


**Fig. 5** Stereoisogram of Type IV for a prismane derivative with the constitution  $H_5A$ , which exhibits  $C_s$ . The symbol A represents an achiral proligand

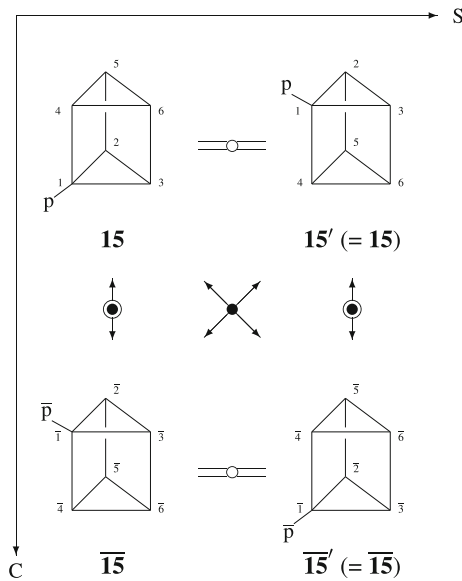


**Fig. 6** Stereoisogram of Type II for a prismane derivative with the constitution  $H_5p$  or  $H_5\bar{p}$ , which exhibits  $C_1$ . The symbols p and  $\bar{p}$  represent a pair of enantiomeric proligands when detached

The stereoisogram of Type IV for the  $C_s$ -derivative **18** is shown in Fig. 8 (left). It belongs to the *RS*-stereoisomeric group  $C_{1\sigma\tilde{\sigma}\tilde{I}}$  (Eq. 31), which is a subgroup of the *RS*-stereoisomeric group  $D_{3h\tilde{\sigma}\tilde{I}}$  (Eq. 6). See Eq. 17.

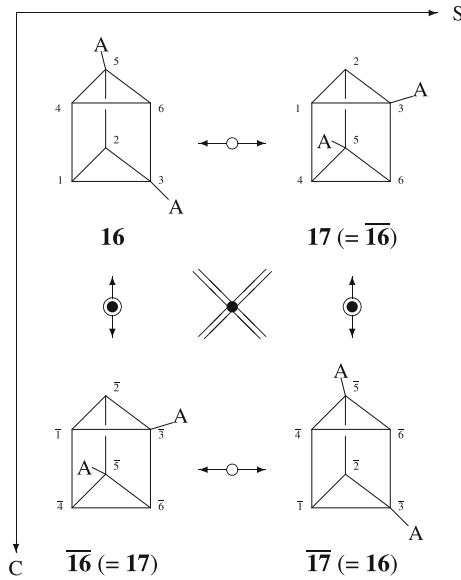


**Fig. 7** Stereoisogram of Type I for prismane derivatives with the constitution  $H_4A_2$ , which exhibits the symmetry of  $C_2$ . The stereoisogram of Type I belongs to the ligand-reflection group  $C_{2i}$ , which is a subgroup of  $D_{3i}$  ( $C D_{3h\bar{i}}$ )

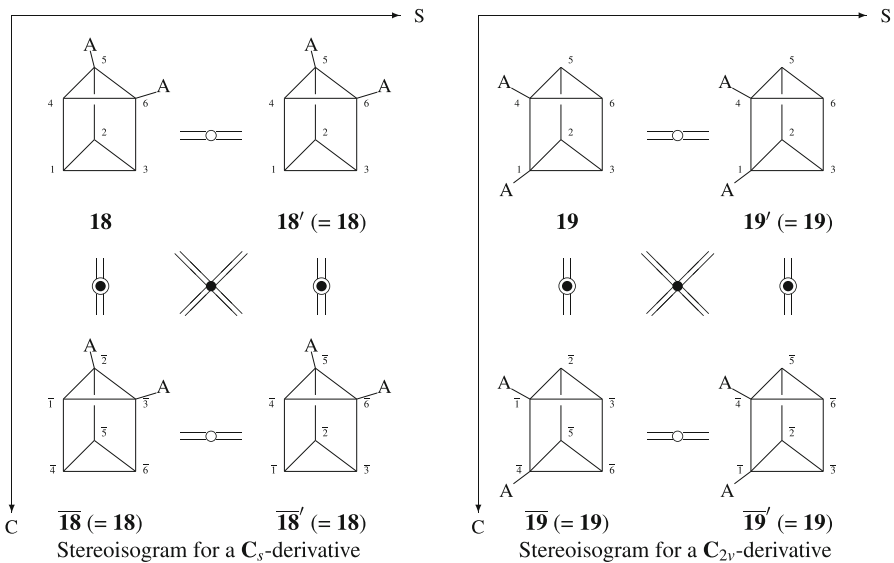


**Fig. 8** Stereoisograms of Type IV for prismane derivatives with the constitution  $H_4A_2$ , i.e., a  $C_5$ -derivative (left) and a  $C_{2v}$ -derivative (right). The symbol A represents an achiral ligand

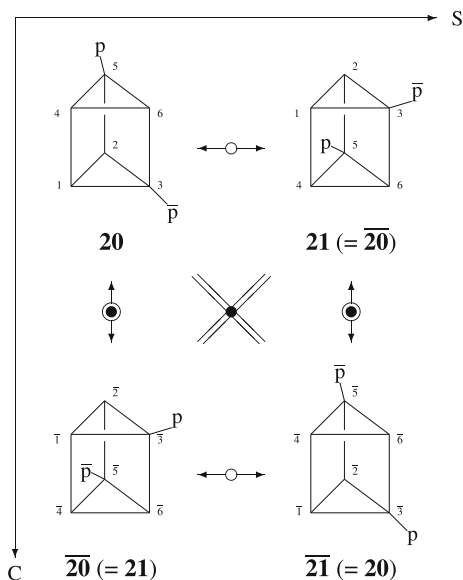


**Fig. 9** Stereoisogram of Type I for a prismane derivative with the constitution  $H_4p\bar{p}$ , which exhibits the symmetry of  $C_1$ . The stereoisogram of Type I belongs to the ligand-reflection group  $C_2$ , which is a subgroup of  $D_{3\hat{I}} (\subset D_{3h\bar{\sigma}\hat{I}})$

The stereoisogram of Type IV for the  $C_{2v}$ -derivative **19** is shown in Fig. 8 (right). It belongs to the *RS*-stereoisomeric group  $C_{2v\bar{\sigma}\hat{I}}$  shown below:

$$C_{2v\bar{\sigma}\hat{I}} = \{I, C_{2(1)}, \sigma_h, \sigma_{v(1)}, \hat{I}, \hat{C}_{2(1)}, \tilde{\sigma}_h, \tilde{\sigma}_{v(1)}\} \tag{34}$$

$$\sim \{(1)(2)(3)(4)(5)(6), (1\ 4)(2\ 6)(3\ 5), \overline{(1\ 4)(2\ 5)(3\ 6)}, \overline{(1)(2\ 3)(4)(5\ 6)}, \overline{(1)(2)(3)(4)(5)(6)}, \overline{(1\ 4)(2\ 6)(3\ 5)}, (1\ 4)(2\ 5)(3\ 6), (1)(2\ 3)(4)(5\ 6)\}, \tag{35}$$

which is a subgroup of the *RS*-stereoisomeric group  $D_{3h\bar{\sigma}\hat{I}}$  (Eq. 6). See Eq. 17.

### 3.3 Prismane derivatives with a pair of substituents enantiomeric in isolation

The [4,0,0,0,0,0;1,1,0,0]-row of Table 1 of Part 1 indicates that there are one pair of enantiomeric  $C_1$ -derivatives, two  $C_s$ -derivatives, one  $C'_s$ -derivative, which have the constitution of  $H_4p\bar{p}$ .

The pair of enantiomeric  $C_1$ -derivatives (**20/20**) corresponds to a quadruplet of *RS*-stereoisomers which are contained in a stereoisogram of Type I, as shown in Fig. 9. Compare this with the stereoisograms of Type I shown in Figs. 4 and 7. The stereoisogram of Type I (Fig. 9) belongs to the ligand-reflection group  $C_2$  (Eq. 27), which is a subgroup of the ligand-reflection group  $D_{3\hat{I}}$  (Eq. 5). See also Eq. 15 for Type I.

The two  $C_s$ -derivatives (**22** and **23**) are combined together to construct a stereoisogram of Type V, as shown in Fig. 10 (left). Along the S-axis, **22** and **23** are *RS*-diastereomeric to each other, so that they exhibit extended pseudoasymmetry as



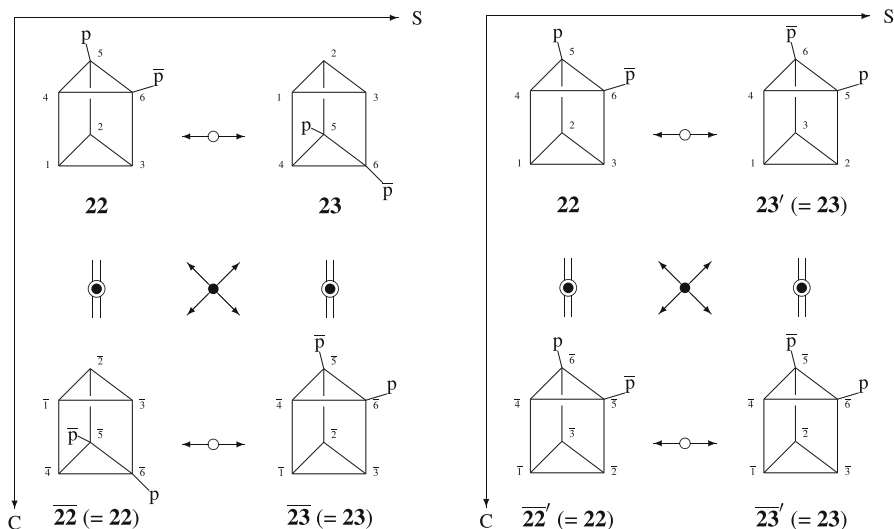


**Fig. 10** Equivalent stereoisograms of Type V for a prismane derivative with the constitution  $H_4p\bar{p}$ , which exhibits the symmetry of  $C_s$ . The left diagram is based on the mode of numbering due to a selection of representatives,  $I$ ,  $\sigma_h$ ,  $\tilde{\sigma}_h$ , and  $\hat{I}$ , while the right diagram is based on the mode of numbering due to another selection of representatives,  $I$ ,  $\sigma_{v(1)}$ ,  $\tilde{\sigma}_{v(1)}$ , and  $\hat{I}$ . The stereoisogram of Type V belongs to the point group  $C_s$ , which is a subgroup of  $D_{3h}$  ( $C D_{3h}\tilde{\sigma}\hat{I}$ )

discussed later. The promolecule **22** (or **23**) is fixed (stabilized) under the action of the point group  $C_s$  (Eq. 33), which is a subgroup of the point group  $D_{3h}$  (Eq. 1). Along a similar line to the Type V stereoisogram of Fig. 4, the promolecule (**22** or **23**) generated by  $\sigma_h$  is homomeric to the original promolecule (**22** or **23**).

It should be noted that the four promolecules collected in Fig. 10 (left) are generated in accord with the representatives,  $I$ ,  $\sigma_h$ ,  $\tilde{\sigma}_h$ , and  $\hat{I}$ , which appear in the coset decomposition (Eq. 6) or in the factor group (Eq. 10). Such a homomeric relationship is directly confirmed by another selection of representatives  $I$ ,  $\sigma_{v(1)}$ ,  $\tilde{\sigma}_{v(1)}$ , and  $\hat{I}$ , as shown in Fig. 10 (right). This selection corresponds to the renumbering of substitution positions as found in Fig. 10 (right). Thereby, both **22** and **22'** (or **23** and **23'**) represent the same structure, where the identification between them does not require no further operation for confirming such a homomeric relationship. In other words, the  $C_s$ -symmetry of **22** or **23** can be directly determined by Fig. 10 (right).

The  $C'_s$ -derivative (**24**) constructs a quadruplet of  $RS$ -stereoisomers, which gives a stereoisogram of Type IV, as shown in Fig. 11. The quadruplet is degenerated into a single achiral promolecule. The  $C'_s$ -derivative (**24**) is fixed (stabilized) under the action of the following  $RS$ -stereoisomeric group  $C_{1\sigma\tilde{\sigma}2}$ :

$$C_{1\sigma\tilde{\sigma}2} = \{I, \sigma_h, \tilde{\sigma}_{v(1)}, \hat{C}_{2(1)}\} \quad (36)$$

$$\sim \{(1)(2)(3)(4)(5)(6), \overline{(1\ 4)(2\ 5)(3\ 6)}, \\ (1)(2\ 3)(4)(5\ 6), \overline{(1\ 4)(2\ 6)(3\ 5)}\}, \quad (37)$$

which is a subgroup of the  $RS$ -stereoisomeric group  $D_{3h}\tilde{\sigma}\hat{I}$  (Eq. 6). See Eq. 17.

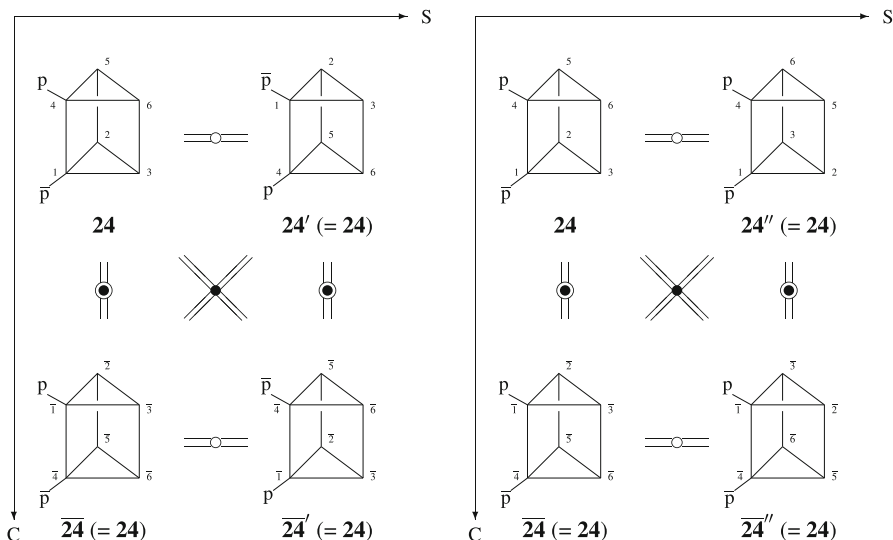


**Fig. 11** Equivalent stereoisograms of Type IV for a prismane derivative with the constitution  $H_4p\bar{p}$ , which exhibits  $C'_s$ . The left diagram is based on the mode of numbering due to a selection of representatives,  $I, \sigma_h, \tilde{\sigma}_h$ , and  $\hat{I}$ , while the right diagram is based on the mode of numbering due to another selection of representatives,  $I, \sigma_h, \tilde{\sigma}_{v(1)}$ , and  $\hat{C}_{2(1)}$

It should be noted that the four promolecules collected in Fig. 11 (left) are generated in accord with the representatives,  $I, \sigma_h, \tilde{\sigma}_h$ , and  $\hat{I}$ , which appear in the coset decomposition (Eq. 6) or in the factor group (Eq. 10). Such a homomeric relationship is directly confirmed by another selection of representatives  $I, \sigma_h, \tilde{\sigma}_{v(1)}$ , and  $\hat{C}_{2(1)}$ , as shown in Fig. 11 (right). This selection corresponds to the renumbering of substitution positions as found in Fig. 11 (right). Thereby, the four promolecules contained in the stereoisogram shown in Fig. 11 (right) represent the same structure, so that the identification between them does not require no further operation for confirming such a homomeric relationship as necessary in Fig. 11 (left).

### 3.4 Prismane derivatives with two chiral substituents ( $H_4p^2$ or $H_4\bar{p}^2$ )

The [4,0,0,0,0,0;2,0,0,0]-row of Table 1 of Part 1 indicates that there are one pair of enantiomeric  $C_1$ -derivatives (due to the term  $1 \times \frac{1}{2}(H^4p^2 + H^4\bar{p}^2)$ ) and three pairs of enantiomeric  $C_2$ -derivatives (due to the term  $3 \times \frac{1}{2}(H^4p^2 + H^4\bar{p}^2)$ ).

The pair of enantiomeric  $C_1$ -derivatives ( $25/25$ ) generates a stereoisogram of Type II shown in Fig. 12, which belongs to the  $RS$ -permutation group  $C_{1\bar{\sigma}}$  (Eq. 29). Note that the hierarchy of subgroups is found to be:  $C_{1\bar{\sigma}}$  (Eq. 29)  $\subset$   $D_{3\bar{\sigma}}$  (Eq. 4)  $\subset$   $D_{3h\bar{\sigma}\hat{I}}$  (Eq. 6) for the  $RS$ -permutation groups, which provide us with a basis for determining Type II stereoisograms because of Eq. 14.

Among the three pairs of  $C_2$ -derivatives having the constitution  $H_4p^2$  or  $H_4\bar{p}^2$ , one pair of  $C_2$ -derivatives ( $26/26$ ) exhibits Type II character, as shown in Fig. 13. The resulting stereoisogram (Fig. 13) belongs to the following  $RS$ -permutation group:

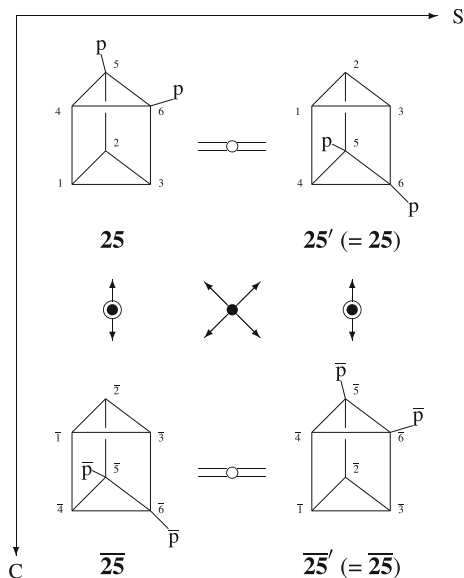


**Fig. 12** Stereoisogram of Type II for a prismane derivative with the constitution  $H_4p^2$  or  $H_4\bar{p}^2$ , which exhibits  $C_1$ . The symbols  $p$  and  $\bar{p}$  represent a pair of enantiomeric proligands when detached

$$C_{2\bar{\sigma}} = \{I, C_{2(1)}, \tilde{\sigma}_h, \tilde{\sigma}_{v(1)}\} \quad (38)$$

$$\sim \{(1)(2)(3)(4)(5)(6), (1\ 4)(2\ 6)(3\ 5), \\ (1\ 4)(2\ 5)(3\ 6), (1)(2\ 3)(4)(5\ 6)\} \quad (39)$$

The hierarchy of the  $RS$ -permutation groups is found to be:  $C_{2\bar{\sigma}}$  (Eq. 39)  $\subset D_{3\bar{\sigma}}$  (Eq. 4)  $\subset D_{3h\bar{\sigma}\hat{I}}$  (Eq. 6), so that it provides us with a basis for determining Type II stereoisograms because of Eq. 14.

Among the three pairs of  $C_2$ -derivatives having the constitution  $H_4p^2$  or  $H_4\bar{p}^2$ , the remaining two pairs of  $C_2$ -derivatives (**27/27** and **28/28**) construct a stereoisogram of Type III, as shown in Fig. 14. The resulting stereoisogram (Fig. 13) belongs to the point group  $C_2$ , which is regarded as a subgroup of  $D_3$ , so that the Type III character is confirmed by Eq. 13.

## 4 Discussions

### 4.1 Chirality, $RS$ -stereogenicity, and sclerality

#### 4.1.1 $C/A$ -convention for determining absolute configurations

Although the CIP system for determining  $RS$ -descriptors can be applied to prismane derivatives, it is inconvenient to comprehend gross geometric aspects of prismane derivatives in harmony with stereoisomeric consideration. Hence, a practical procedure of more intuitive nature is desirable to discuss absolute configurations of prismane

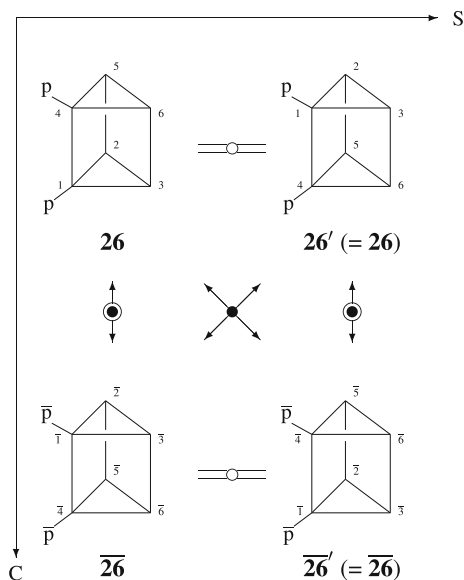


**Fig. 13** Stereoisogram of Type II for a prismane derivative with the constitution  $H_4p^2$  or  $H_4\bar{p}^2$ , which exhibits  $C_2$ . The symbols  $p$  and  $\bar{p}$  represent a pair of enantiomeric proligands when detached

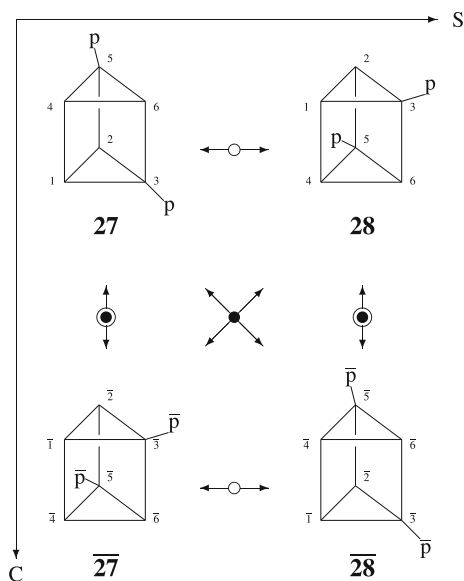


**Fig. 14** Stereoisogram of Type III for a prismane derivative with the constitution  $H_4p^2$  or  $H_4\bar{p}^2$ , which exhibits  $C_2$ . The symbols  $p$  and  $\bar{p}$  represent a pair of enantiomeric proligands when detached

derivatives. We here propose a convention which is a combination of the von Baeyer system for naming polycyclic compounds [37] with the  $C/A$  convention for giving  $C/A$ -descriptors to trigonal prismatic complexes (IR-9.3.4.9 of [1]).

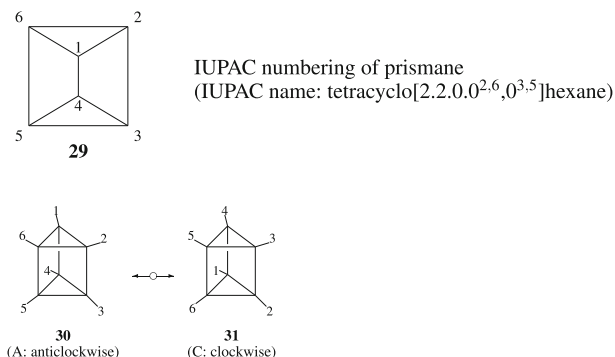


**Fig. 15** IUPAC locant numbering of prismane (*top*) and two modes of numbering adopted in the *C/A*-convention for characterizing absolute configurations of prismane derivatives (*bottom*). According to the stereoisogram approach, the numbered skeletons for the *C/A*-convention are regarded as being in an *RS*-diastereomeric relationship, not in an enantiomeric relationship

The numbering of the IUPAC name of prismane, i.e., tetracyclo[2.2.0.0<sup>2,6</sup>.0<sup>3,5</sup>]hexane, is adopted to name a given prismane derivative in terms of the von Baeyer system of the IUPAC nomenclature [37]. The name of a prismane derivative contains a set of locant numbers for substituents (the top diagram of Fig. 15). After two prismane derivatives having the same 2D structure (or graph) are characterized by the same von Baeyer name, the resulting set of locant numbers (**29**) is applied to the two modes of numbering shown in the bottom diagram of Fig. 15, which are selected to differentiate *RS*-diastereomers corresponding to the 2D structure (**29**), i.e., **30** and **31**. Note that the two modes of numbering are *not* concerned with a pair of enantiomers in accord with the stereoisogram approach. Then, an *A* or *C*-descriptor is assigned by viewing the trigonal prism from above the preferred triangular face (containing vertices 1, 2, and 6) and noting the ascending order of numbers (3, 4, and 5) for the less preferred triangular face. The anticlockwise order (**30**) is characterized by an *A*-descriptor, while the clockwise order (**31**) is characterized by a *C*-descriptor.

As for an illustrative example, let us examine 1,3-dibromoprismane (1,3-dibromotetracyclo[2.2.0.0<sup>2,6</sup>.0<sup>3,5</sup>]hexane), as shown in Fig. 16. This case is a concrete example of Fig. 7 (Type I). According to the modes of numbering due to Fig. 15, an *A*-descriptor to the derivative **32**, while a *C*-descriptor to the derivative **33**. The assignment of the *A/C*-descriptors is concerned with the *RS*-diastereomeric relationship between **32** and **33** ( $= \overline{32}$ ). The resulting *A/C*-descriptors are then reinterpreted to be given to a pair of enantiomers between **32** and  $\overline{32}$  ( $= \overline{33}$ ) according to the chirality-faithfulness [24].

Another example for naming prismane derivatives is shown in Fig. 17, where a pair of chiral proligands (hydroxylcarboxylmethyl groups) is in an enantiomeric relationship when detached. This case is a concrete example of Fig. 10 (Type V). The resulting pair of prismanes are referred to as 1-*p*-2- $\bar{p}$ -prismane in an abbreviated fashion. Then, an *a*-descriptor to the derivative **34**, while a *c*-descriptor to the derivative **35** according to the modes of numbering due to Fig. 15.

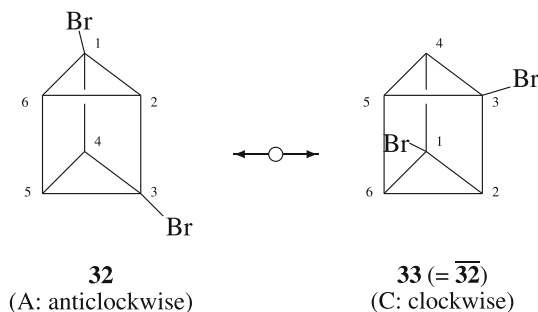


**Fig. 16** (A)-1,3-Dibromoprismantane and (C)-1,3-dibromoprismantane, where the *A/C*-descriptors are given in terms of the convention of Fig. 15. They are *RS*-diastereomeric and enantiomeric to each other

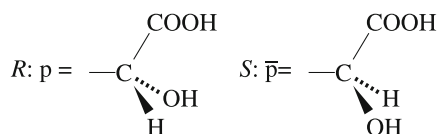
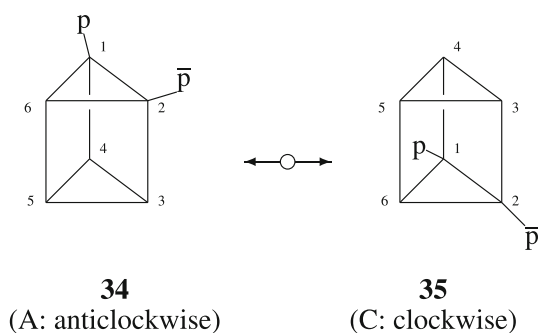


**Fig. 17** (a)- and (c)-1-(*R*-Hydroxylcarboxylmethyl)-2-(*S*-hydroxylcarboxylmethyl) prismane, where the lowercase symbols *a/c* given in place of *A/C* to emphasize that they are achiral. In terms of the convention of Fig. 15, they are *RS*-diastereomeric and achiral (not enantiomeric to each other)

The assignment of the *A/C*-descriptors is based on the *RS*-diastereomeric relationship between **34** and **35** in accord with the stereoisogram approach. Because of the absence of enantiomeric relationships, the resulting *A/C*-descriptors cannot be reinterpreted to be given to enantiomers. Both **34** and **35** are achiral so that the lowercase letters *a/c* are used in place of the uppercase letters *A/C*.

If we obey the conventional methodology of stereochemistry, the case of Fig. 16 is considered to determine an enantiomeric relationship between **32** and  $\overline{32}$  (= **33**), while the case of Fig. 17 is considered to determine a diastereomeric relationship between **34** and **35**. The conventional diastereomeric relationship is not recognized as a pairwise relationship. Moreover, the conventional methodology does not permit the concurrent appearance of enantiomeric relationships and diastereomeric ones in terms of the dichotomy between enantiomeric relationships and diastereomeric ones.

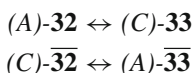
In contrast, both Fig. 16 and Fig. 17 are based on *RS*-diastereomeric relationships as pairwise relationships. The cases shown in Fig. 16 (Type I) and Fig. 17 (Type V) will be discussed below from a common viewpoint of the stereoisogram approach.

#### 4.1.2 Chirality and *RS*-stereogenicity for Type I stereoisograms

Stereoisograms of Type I reveal a misleading principle of the conventional stereochemistry, i.e., preferential consideration of chirality coupled with ignorance of *RS*-stereogenicity. This principle results in preferential consideration of enantiomeric relationships along with ignorance of *RS*-diastereomeric relationships. In other words, the conventional stereochemistry adopts the dichotomy between enantiomeric relationships and diastereomeric ones (cf. [2]). In contrast, the stereoisogram approach [10, 12] concludes that chirality and *RS*-stereogenicity are independent concepts, so that the vertical C-axis and the horizontal S-axis are considered independently even in stereoisograms of Type I.

Let us examine the stereoisogram of Type I (Fig. 7), where **16** and  $\overline{\mathbf{16}}$  are usually recognized to be a pair of enantiomers. Such a stereoisogram of Type I is characterized to be chiral, *RS*-stereogenic, and ascleral (the stereoisogram index  $[-, -, a]$ ) [10, 12]. The presence of enantiomers stems from chirality (cf. Table 1). This recognition depends upon the inspection along the C-axis of the stereoisogram of Type I (Fig. 7). From a viewpoint of the stereoisogram approach, the inspection along S-axis of Fig. 7 is also important, so that **16** and **17** ( $= \overline{\mathbf{16}}$ ) are recognized to be a pair of *RS*-diastereomers. The presence of *RS*-diastereomers stems from *RS*-stereogenicity.

The emphasis of the S-axis of a stereoisogram (i.e., *RS*-stereogenicity) is a crux for the newly-proposed convention for giving *A/C*-descriptors, e.g., (*A*)-1,3-dibromoprismene (**32**) and (*C*)-1,3-dibromoprismene **33** ( $= \overline{\mathbf{32}}$ ), as described in Fig. 16. Note that Fig. 16 can be regarded as the selection of the S-axis from the corresponding stereoisogram of Type I (e.g., Fig. 7). The assignment of these *A/C*-descriptors is concerned with the *RS*-diastereomeric relationship between **32** and **33** ( $= \overline{\mathbf{32}}$ ), not with the enantiomeric relationship between **32** and  $\overline{\mathbf{32}}$  ( $= \mathbf{33}$ ). More clearly speaking, a pair of *A*- and *C*-descriptors is assigned in a pairwise fashion:



even though the *RS*-diastereomeric relationship and the enantiomeric one overlap each other in the case of a Type I stereoisogram.

Let us next examine the other stereoisogram of Type I (Fig. 9), where **20** and  $\overline{\mathbf{20}}$  are usually recognized to be a pair of enantiomers along the C-axis. According to the stereoisogram approach, a pair of *RS*-diastereomers (**20/21** ( $= \mathbf{20}/\overline{\mathbf{20}}$ )) is taken into consideration. In other words, the S-axis of the stereoisogram of Type I (Fig. 9) plays an important role in the newly-proposed convention for giving *A/C*-descriptors. The two promolecules along the S-axis (i.e., **20** and **21** as *RS*-diastereomers) are compared with the modes of numbering (**30** and **31**) shown in Fig. 15 so that their configura-

tions are determined to be (*A*)-1-*p*-3- $\bar{p}$ -prismane for **20** and (*C*)-1-*p*-3- $\bar{p}$ -prismane for **21** (=  $\overline{\mathbf{20}}$ ).

#### 4.1.3 Extended pseudoasymmetry

Let us compare the stereoisogram of Type V shown in Fig. 10 with the scheme shown in Fig. 17, where the latter scheme (Fig. 17) can be regarded as the upper half of the stereoisogram of Fig. 10. A pair of *A*- and *C*-descriptors is assigned in a pairwise fashion:

$$(a)\text{-}\mathbf{34}(=\overline{\mathbf{34}}) \leftrightarrow (c)\text{-}\mathbf{35}(=\overline{\mathbf{33}})$$

where lowercase letters *a* and *c* are used for the sake of compatibility for *RS*-descriptors. The scheme of Fig. 17 for assigning *A/C*-descriptors shows that this case is an extension of a pseudoasymmetric case for assigning *RS*-descriptors, where the prismane skeleton is adopted in place of a usual single-atom center.

Let us next compare the stereoisogram of Type I shown in Fig. 7 with the scheme shown in Fig. 16, where the latter scheme (Fig. 16) can be regarded as the upper half of the stereoisogram of Fig. 7. The scheme of Fig. 16 for assigning *A/C*-descriptors shows that this case is an extension of a tetrahedral asymmetric case for assigning *RS*-descriptors, where the prismane skeleton is adopted in place of a usual single-atom center.

According to the stereoisogram approach, the terms asymmetry and pseudoasymmetry are revised to give the following schemes:

$$\text{asymmetry} \text{ --- } \boxed{\text{chiral}}, \boxed{\boxed{RS\text{-stereogenic}}}, \text{ and ascleral (Type I)} \quad (40)$$

$$\text{pseudoasymmetry} \text{ --- } \boxed{\text{achiral}}, \boxed{\boxed{RS\text{-stereogenic}}}, \text{ and scleral (Type V)} \quad (41)$$

When the stereoisogram approach puts stress on *A/C*-descriptors or *RS*-descriptors, it emphasizes the *S*-axis of a stereoisogram not only for (extended) pseudoasymmetric cases (Type V) but also for (extended) asymmetric cases (Type I). This emphasis is shown by a double frame for surrounding the term *RS*-stereogenic (Eqs. 40, 41). When the stereoisogram approach puts stress on geometric aspects, it emphasized the *C*-axis of a stereoisogram (i.e., chirality) not only for (extended) pseudoasymmetric cases (Type V) but also for (extended) asymmetric cases (Type I). The terms chirality/achirality correspond to the terms enantiomeric/self-enantiomeric relationships (Table 1). This emphasis is shown by a single frame for surrounding the term chiral (Eq. 40) or achiral (Eq. 41).

This methodology of the stereoisogram approach shows sharp contrast to the conventional stereochemistry, in which chirality (cf. the *C*-axis in the stereoisogram approach) is only taken into consideration in such (extended) asymmetric cases (Type I), as shown by a double frame for surrounding the term chiral (Eq. 42) as follows:



asymmetry —  $\boxed{\text{chiral}}$ , *RS*-stereogenic, and ascleral (Type I) (42)

pseudoasymmetry — achiral,  $\boxed{[RS\text{-}]stereogenic}$ , and scleral (Type V) (43)

Note that *RS*-stereogenicity and asclerality in Eq. 42 are neglected in the conventional stereochemistry. This preference of chirality in such (extended) asymmetric cases (Type I in Eq. 42) is inconsistent to the preference of stereogenicity for (extended) pseudoasymmetric cases (Type V in Eq. 43), although the conventional stereogenicity is different from the *RS*-stereogenicity. Thus, the criterion for assigning *A/C*-descriptors or *RS*-descriptors is different between Type I in Eq. 42 and Type V in Eq. 42 in the conventional stereochemistry.

#### 4.1.4 *A/C*-descriptors for Type II and Type III cases

The Type II cases shown in Figs. 12 and 13 cannot be named by the convention described in Fig. 15, because both **30** and **31** give promolecules identical with each other. When *p* and  $\bar{p}$  are considered to be equal to the proligands shown in Fig. 17, the pair of enantiomers **25/25** (Fig. 12) is named as follows:

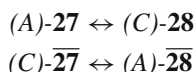
1-(*R*-Hydroxylcarboxylmethyl)-2-(*R*-hydroxylcarboxylmethyl)prismane and  
1-(*S*-Hydroxylcarboxylmethyl)-2-(*S*-hydroxylcarboxylmethyl)prismane,

where they are differentiated by the absolute configurations of the proligands. Similarly, the pair of enantiomers **26/26** (Fig. 13) is named as follows:

1-(*R*-Hydroxylcarboxylmethyl)-4-(*R*-hydroxylcarboxylmethyl)prismane and  
1-(*S*-Hydroxylcarboxylmethyl)-4-(*S*-hydroxylcarboxylmethyl)prismane,

where they are differentiated by the absolute configurations of the proligands.

The Type III case shown in Fig. 14 can be named by the convention described in Fig. 15. i.e., (*A*)-1,3-di-*p*-prismane for **27**, (*C*)-1,3-di-*p*-prismane for **28**, (*C*)-1,3-di- $\bar{p}$ -prismane for  $\overline{\mathbf{27}}$ , and (*A*)-1,3-di- $\bar{p}$ -prismane for  $\overline{\mathbf{28}}$ . Note that the selection of Fig. 15 as a basis of the *C/A*-convention can be regarded as the preferential selection of the *S*-axis from the corresponding stereoisogram of Type III (e.g., Fig. 14). The pairwise assignment of these *A/C*-descriptors is concerned with the *RS*-diastereomeric relationship between **27** and **28** or between  $\overline{\mathbf{27}}$  and  $\overline{\mathbf{28}}$ , not with the enantiomeric relationship between **27** and  $\overline{\mathbf{27}}$  or between **28** and  $\overline{\mathbf{28}}$ . Thus, a pair of *A*- and *C*-descriptors is assigned in a pairwise fashion:



This type of pairing is clearly supported by the proligand-promolecule model proposed by Fujita [7, 29], because the comparison between **27** and **28** (or between  $\overline{\mathbf{27}}$  and  $\overline{\mathbf{28}}$ ) is concerned with promolecules of the same constitution, e.g., *p*'s (or  $\bar{p}$ 's) in the case of Fig. 14.

**Table 2** Relational terms which correspond to the attributive terms for discussing prochirality, pro-*RS*-stereogenicity, and proslclerality

	Relationship between members	Attribute of an orbit	Attribute of a promolecule
Along the C-axis	Enantiotopic	Enantiospheric	Prochiral
Along the S-axis	<i>RS</i> -diastereotopic	<i>RS</i> -enantiotopic	Pro- <i>RS</i> -stereogenic
Along the diagonal direction	Holantopic	Enantiocercal	Proslcleral

## 4.2 Prochirality, pro-*RS*-stereogenicity, and proslclerality

The concept of sphericities has been proposed by Fujita to determine prochirality [29,38,39]. The concept of tropicities proposed by Fujita [36] has been restricted into the concept of *RS*-tropicities to determine pro-*RS*-stereogenicity [20]. These two concepts have been discussed in an integrated fashion by following the stereoisogram approach so that the concept of *coset-representation (CR) type* has been proposed by Fujita [20] to comprehensively determine prochirality, pro-*RS*-Stereogenicity, and proslclerality. As illustrative examples, this subsection is devoted to discuss the prochirality, pro-*RS*-Stereogenicity, and proslclerality of prismane derivatives.

### 4.2.1 Attributive terms versus relational terms

In the following discussions for intramolecular aspects of stereoisograms, we have mainly used attributive terms for specifying orbits (equivalence classes), e.g., sphericities [29,38,39], tropicities [20], and cercalities, in harmony with the terms for discussing intermolecular aspects (Table 1) [10,12]. Because stereochemistry has put emphasis on such relational terms as *enantiomeric* (for intermolecular aspects) and *enantiotopic* (for intramolecular aspects), relational terms corresponding to the attributive terms are desirable to be coined for the purpose of spreading the stereoisogram approach. They are summarized in Table 2, where several terms have already been defined in previous papers [21,22]. It should be noted that the relational term *enantiotopic* is used in a purely geometric meaning.

### 4.2.2 Geometric prochirality in stereoisograms of Type V

In the stereoisogram approach developed by Fujita [10,12], the term *prochirality* is used in a purely geometric meaning (i.e., *geometric prochirality*), because the conventional “prochirality” is used in different, sometimes contradictory ways as shown in [41]. Roughly speaking, the conventional “prochirality” has mixed up two conceptually independent matters, i.e., geometric prochirality [29,38,39] and pro-*RS*-stereogenicity [20,36], which have been integrated by Fujita [20] as part of the stereoisogram approach.

Geometric prochirality for prismane derivatives has been discussed in Part I of this series by following the unit-subduced-cycle-index (USCI) approach [29], where the concept of enantiosphericity plays a decisive role [32,33,38].

Let us examine the stereoisogram of Type V shown in Fig. 10. Geometrically speaking, the chiral proligands  $p$  and  $\bar{p}$  of **22** (or **23**) construct an enantiospheric orbit  $C_s/(C_1)$ . Hence, **22** (or **23**) is concluded to be prochiral in a purely geometric meaning [32,33,38].

By following the stereoisogram approach, the promolecule **22** (or **23**) belongs to a point group  $C_s$  (the same as the point group  $C_s$  of a narrower sense), which is a subgroup of the point group  $D_{3h}$  ( $\subset D_{3h\bar{\sigma}\bar{\tau}}$  (Eq. 6)). By following Eq. 16, the global symmetry of **22** (or **23**) is determined to be Type V ( $[a, -, -]$ ). The group  $C_s$  is symbolically represented by a global symmetry  $G_V$  from a viewpoint of the stereoisogram approach. The local symmetry of  $p$  (or  $\bar{p}$ ) in **22** (or **23**) is determined to be  $C_1$  ( $= (1)(2)(3)(4)(5)(6)$ ), which is a subgroup of  $D_3$ . By following Eq. 13, the local symmetry of  $p$  (or  $\bar{p}$ ) is determined to be Type III ( $[-, -, -]$ ). The group  $C_1$  is symbolically represented by a local symmetry  $H_{III}$  from a viewpoint of the stereoisogram approach.

The orbit of  $\{p, \bar{p}\}$  is governed by  $C_s/(C_1)$ , which is represented to be a symbolic coset representation  $G_V/(H_{III})$  and characterized by a coset-representation (CR) index  $\frac{[a, -, -]}{[-, -, -]}$ . The achirality of  $[a, -, -]$  and the chirality of  $[-, -, -]$  indicates the enantiosphericity of the orbit of  $\{p, \bar{p}\}$ , which determines the prochirality of **22** (or **23**). This criterion based on the CR index gives the conclusion consistent to the geometric consideration based on the concept of sphericity (cf. Part I of this series).

It should be emphasized that the determination of the prochirality of **22** (or **23**) is concerned with the achirality appearing in the vertical C-axis of the stereoisogram of Type V (Fig. 10). This means that the differentiation between  $p$  and  $\bar{p}$  of **22** (or **23**) is possible under a chiral condition, so that **22** (or **23**) is capable of generating either of the corresponding chiral products (enantiomers).

#### 4.2.3 Pro-*RS*-stereogenicity in stereoisograms of Type II

Let us examine the stereoisogram of Type II shown in Fig. 12. Geometrically speaking, the two chiral proligands of the same kind  $p$ 's of **25** (or  $\bar{p}$ 's of  $\overline{25}$ ) separately construct two one-membered hemispheric orbits  $C_1/(C_1)$ .

By following the stereoisogram approach, the promolecule **25** (or  $\overline{25}$ ) belongs to an *RS*-permutation group  $C_{1\bar{\sigma}}$  (Eq. 29), which is a subgroup of the *RS*-permutation group  $D_{3\bar{\sigma}}$  (Eq. 4). By following Eq. 14, the global symmetry of **25** (or  $\overline{25}$ ) is determined to be Type II ( $[-, a, -]$ ). The group  $C_{1\bar{\sigma}}$  is symbolically represented by a global symmetry  $G_{II}$  from a viewpoint of the stereoisogram approach. The local symmetry of  $p$  in **25** (or  $\bar{p}$  in  $\overline{25}$ ) is determined to be  $C_1$  ( $= (1)(2)(3)(4)(5)(6)$ ), which is a subgroup of  $D_3$ . By following Eq. 15, the local symmetry of  $p$  (or  $\bar{p}$ ) is determined to be Type III ( $[-, -, -]$ ). The group  $C_1$  is symbolically represented by a local symmetry  $H_{III}$  from a viewpoint of the stereoisogram approach.

The orbit of  $\{2p\}$  (or  $\{2\bar{p}\}$ ) is governed by  $C_{1\bar{\sigma}}/(C_1)$ , which is symbolically represented to be a coset representation  $G_{II}/(H_{III})$  and characterized by a CR index  $\frac{[-, a, -]}{[-, -, -]}$ . The *RS*-astereogenicity (*RS*-non-stereogenicity) of  $[-, a, -]$  and the *RS*-stereogenic-

ity of  $[-, -, -]$  indicates the *RS*-enantiotropicity of the orbit of  $\{2p\}$  (or  $\{2\bar{p}\}$ ), which determines the pro-*RS*-stereogenicity of **25** (or  $\overline{\mathbf{25}}$ ).

It should be emphasized that the determination of the pro-*RS*-stereogenicity of **25** (or  $\overline{\mathbf{25}}$ ) is concerned with the *RS*-astereogenicity (*RS*-non-stereogenicity) appearing in the horizontal S-axis of the stereoisogram of Type II (Fig. 12). This means that the differentiation between the two  $p$ 's of **25** (or the two  $\bar{p}$ 's of  $\overline{\mathbf{25}}$ ) is possible in a nomenclature basis, so that **25** (or  $\overline{\mathbf{25}}$ ) is capable of producing *RS*-diastereomers of opposite *A/C*-descriptors. Geometrically speaking, the two  $p$ 's of **25** (or the two  $\bar{p}$ 's of  $\overline{\mathbf{25}}$ ) are already separated to be inequivalent.

As for the stereoisogram of Type II shown in Fig. 13, the global symmetry of the promolecule **26** (or  $\overline{\mathbf{26}}$ ) is determined to be an *RS*-permutation group  $C_{2\bar{\sigma}}$  (Eq. 39), which is a subgroup of the *RS*-permutation group  $D_{3\bar{\sigma}}$  (Eq. 4). The group  $C_{2\bar{\sigma}}$  is symbolically represented by a global symmetry  $G_{II}$  from a viewpoint of the stereoisogram approach. On the other hand, the local symmetry of the  $p$  in **26** (or of the  $\bar{p}$  in  $\overline{\mathbf{26}}$ ) is determined to be  $C_{1\bar{\sigma}}$  (Eq. 29), which is a subgroup of the *RS*-permutation group  $D_{3\bar{\sigma}}$  (Eq. 4). The group  $C_{1\bar{\sigma}}$  is symbolically represented by a local symmetry  $H_{II}$  from a viewpoint of the stereoisogram approach. Hence, the orbit of  $\{2p\}$  (or  $\{2\bar{p}\}$ ) is governed by  $C_{2\bar{\sigma}}(/C_{1\bar{\sigma}})$ , which is symbolically represented to be a coset representation  $G_{II}(/H_{II})$  and characterized by a CR index  $\begin{bmatrix} -, a, - \\ -, a, - \end{bmatrix}$ . It follows that the orbit of  $\{2p\}$  in **26** (or the orbit of  $\{2\bar{p}\}$  in  $\overline{\mathbf{26}}$ ) does not characterized by prochirality nor by pro-*RS*-stereogenicity.

#### 4.2.4 Prosclerality in stereoisograms of Type I

Let us examine the stereoisogram of Type I shown in Fig. 9. Geometrically speaking, the chiral proligands  $p$  and  $\bar{p}$  of **20** (or  $\overline{\mathbf{20}}$ ) construct two one-membered hemispheric orbit ( $C_1(/C_1)$ ) separately. Hence, **20** (or  $\overline{\mathbf{20}}$ ) is already chiral and not characterized in terms of prochirality in a purely geometric meaning [32,33,38].

By following the stereoisogram approach, the promolecule **20** (or  $\overline{\mathbf{20}}$ ) belongs to a ligand-reflection group  $C_2$  (Eq. 27), which is a subgroup of the ligand-reflection group  $D_{3\bar{\gamma}}$  (Eq. 5). By referring to Eq. 15, the global symmetry of **20** (or  $\overline{\mathbf{20}}$ ) is determined to be Type I ( $[-, -, a]$ ). The group  $C_2$  is symbolically represented by a global symmetry  $G_I$  from a viewpoint of the stereoisogram approach. The local symmetry of  $p$  in **20** (or  $\bar{p}$  in  $\overline{\mathbf{20}}$ ) is determined to be  $C_1 (= (1)(2)(3)(4)(5)(6))$ , which is a subgroup of  $D_3$ . By following Eq. 13, the local symmetry of  $p$  (or  $\bar{p}$ ) is determined to be Type III ( $[-, -, -]$ ), where the group  $C_1$  is symbolically represented by a local symmetry  $H_{III}$  from a viewpoint of the stereoisogram approach.

The orbit of  $\{p, \bar{p}\}$  is governed by  $C_2(/C_1)$ , which is represented to be a symbolic coset representation  $G_I(/H_{III})$  and characterized by a CR index  $\begin{bmatrix} -, -, a \\ -, -, - \end{bmatrix}$ . The asclerality of  $[-, -, a]$  and the sclerality of  $[-, -, -]$  indicates the enantiocecality of the orbit of  $\{p, \bar{p}\}$ , which determines the prosclerality of **20** (or  $\overline{\mathbf{20}}$ ). The term *enantiocecal* (as well as *homocercal* and *hemicercal*) is coined (*-cercal*: tailed) to denote an ascleral/scleral case (as well as an ascleral/ascleral case and a scleral/scleral case) in analogy to the terms of sphericities and those of *RS*-tropicities which support membership criteria for prochirality [29,38,39] and pro-*RS*-stereogenicity [20]. Just as the

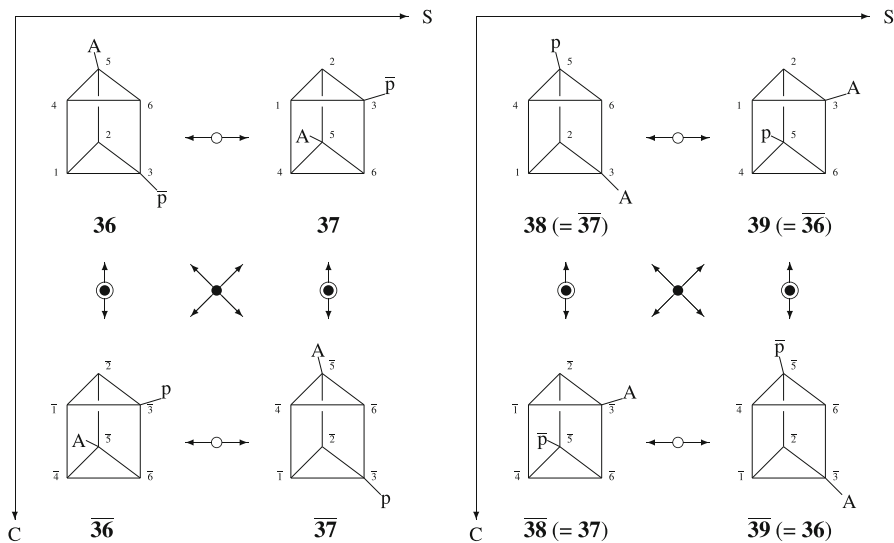


**Fig. 18** Equivalent stereoisograms of Type III for a prismane derivative with the constitutions  $H_4A\bar{p}$  and  $H_4Ap$ , which are produced from the stereoisogram of Type I with the constitution  $H_4p\bar{p}$  (Fig. 9). All of these promolecules exhibit the symmetry of  $C_1$

membership criteria for pro-*RS*-stereogenicity have been redefined by relational terms [22], the concept of proslcerality based on the attributive term *enantiocercal* can be redefined by such an appropriate relational term as *holantitopic* (corresponding to the term *holantimeric*), as summarized in Table 2.

It should be emphasized that the determination of the proslcerality of **20** (or  $\bar{\mathbf{20}}$ ) is concerned with the asclerality appearing in the diagonal direction of the stereoisogram of Type I (Fig. 9). The differentiation between  $p$  and  $\bar{p}$  of **20** (or  $\bar{\mathbf{20}}$ ) is capable of generating either of the corresponding chiral products (holantimers). This differentiation (by the attack of an achiral proligand A) corresponds to the process of converting a stereoisogram of Type I into two stereoisograms of Type III, which are illustrated in Fig. 18. Note that the replacement of the proligand  $p$  by A in **20** generates the left stereoisogram of Fig. 18, while the replacement of the proligand  $\bar{p}$  by A in **20** generates the right stereoisogram of Fig. 18. These two stereoisograms are equivalent to each other, so that they show substitution criteria for determining proslcerality in analogy to substitution criteria based on stereoisograms to determine prochirality and pro-*RS*-stereogenicity [21]. The diagonal equality symbols in Fig. 9 are changed into diagonal double-headed arrows in Fig. 18.

#### 4.2.5 Superposition of prochirality and pro-*RS*-stereogenicity in stereoisograms of Type IV

Let us examine the stereoisogram of Type IV shown in Fig. 8 (left). Geometrically speaking, the two achiral proligands A's of **18** construct a two-membered enantiospheric orbit  $C_s/(C_1)$ . Hence, **18** is concluded to be prochiral in a purely geometric

meaning [32,33,38]. Note that the two A's of the  $C_s(/C_1)$ -orbit are enantiotopic to each other (Table 2).

The orbit of A's of **18** at the same time construct a two-membered *RS*-enantiotropic orbit  $C_{1\bar{\sigma}}(/C_1)$ , where  $C_{1\bar{\sigma}}$  is an *RS*-permutation group represented by Eq. 29. Hence, **18** is concluded to be pro-*RS*-stereogenic [20]. Note that the two A's of the  $C_{1\bar{\sigma}}(/C_1)$ -orbit are *RS*-diastereotopic to each other (Table 2).

It follows that the prochirality and the pro-*RS*-stereogenicity are superposed in the stereoisogram of Type IV shown in Fig. 8 (left). From a viewpoint of the stereoisogram approach, the (geometric) prochirality and the pro-*RS*-stereogenicity are independent to each other. In contrast, the term “prochirality” proposed by Hanson [40] is concluded to mix up the (geometric) prochirality with the pro-*RS*-stereogenicity. Thus, the term “prochirality” is used in the same meaning as the geometric prochirality in discussing geometric aspects, while the same term “prochirality” is used in the same meaning as the pro-*RS*-stereogenicity in assigning *pro-R/pro-S*-descriptors.

By following the stereoisogram approach, the promolecule **18** (or the corresponding stereoisogram of Type IV) belongs to an *RS*-stereoisomeric group  $C_{1\sigma\bar{\sigma}\hat{I}}$  (Eq. 31), which is a subgroup of the *RS*-stereoisomeric group  $D_{3h\bar{\sigma}\hat{I}}$  (Eq. 6). By following Eq. 17, the global symmetry of **18** is determined to be Type IV ( $[a, a, a]$ ). The group  $C_{1\sigma\bar{\sigma}\hat{I}}$  is symbolically represented by a global symmetry  $G_{IV}$  from a viewpoint of the stereoisogram approach.

The local symmetry of A in **18** is determined to be a ligand-reflection group as follows:

$$C_{1\hat{I}} = \{I, \hat{I}\} \quad (44)$$

$$\sim \{(1)(2)(3)(4)(5)(6), \overline{(1)(2)(3)(4)(5)(6)}\}, \quad (45)$$

which is a subgroup of the ligand-reflection group  $D_{3\hat{I}}$  (Eq. 5). By following Eq. 15, the local symmetry of A is determined to be Type I ( $[-, -, a]$ ). The group  $C_{1\hat{I}}$  is symbolically represented by a local symmetry  $H_I$  from a viewpoint of the stereoisogram approach.

The orbit of  $\{2A\}$  is governed by  $C_{1\sigma\bar{\sigma}\hat{I}}(/C_{1\hat{I}})$ , which is represented to be a symbolic coset representation  $G_{IV}/(H_I)$  and characterized by a CR index  $\frac{[a,a,a]}{[-,-,a]}$ . The achirality of  $[a, a, a]$  and the chirality of  $[-, -, a]$  indicates the enantiosphericity of the orbit of  $\{2A\}$ , which determines the prochirality of **18**. This criterion based on the CR index gives the conclusion consistent to the geometric consideration based on the concept of sphericity (cf. Part I of this series). At the same time, the *RS*-astereogenicity of  $[a, a, a]$  and the *RS*-stereogenicity of  $[-, -, a]$  indicates the *RS*-enantiotropicity of the orbit of  $\{2A\}$ , which determines the pro-*RS*-stereogenicity of **18**.

#### 4.2.6 Concurrence in stereoisograms of Type IV

Let us examine the stereoisogram of Type IV shown in Fig. 11 (right). Geometrically speaking, the chiral proligands  $p$  and  $\bar{p}$  of **24** construct an enantiospheric orbit  $C'_s(/C_1)$ . Hence, **24** is concluded to be prochiral in a purely geometric meaning [32,33,38]. Note

that the chiral proligands  $p$  and  $\bar{p}$  of the  $C'_s(/C_1)$ -orbit are enantiotopic to each other (Table 2).

According to the stereoisogram approach, the orbit of  $\{p, \bar{p}\}$  of **24** belongs to a coset representation  $C_{1\sigma\bar{\sigma}2}(/C_{1\bar{\sigma}})$ , which is represented to be a symbolic coset representation  $G_{IV}(/H_{II})$  and characterized by a CR index  $\frac{[a,a,a]}{[-,a,-]}$ . Note that the global symmetry  $C_{1\sigma\bar{\sigma}2}$  (Eq. 37) is an *RS*-stereoisomeric group, which is symbolically represented by a global symmetry  $G_{IV}$  and that the local symmetry  $C_{1\bar{\sigma}}$  (Eq. 29) is an *RS*-permutation group, which is symbolically represented by a local symmetry  $H_{II}$ . The achirality of  $[a, a, a]$  and the chirality of  $[-, a, -]$  determine the enantiosphericity of the orbit of  $\{p, \bar{p}\}$ , which determines the prochirality of **24**.

Let us next examine the four hydrogens of **24** in Fig. 11 (right), where there concurrently emerge all of the three types of attributes, i.e., prochirality, pro-*RS*-stereogenicity, and proscularity, as enumerated as follows:

1. (Prochirality along the C-axis) Geometrically speaking, the four hydrogens (numbered sequentially as 2, 3, 5, and 6) are subdivided into two two-membered orbits, i.e., {2, 5} and {3, 6}, each of which is governed by a coset representation  $C'_s(/C_1)$ . Because the point group  $C'_s (= \{I, \sigma_h\})$  is an achiral subgroup of  $D_{3h}$  and  $C_1 (= \{I\})$  is a chiral subgroup of  $D_{3h}$ , the two orbits {2, 5} and {3, 6} are enantiospheric, so that the promolecule **24** is concluded to be prochiral.

The prochirality concerned with the two enantiospheric orbits {2, 5} and {3, 6} can be confirmed by a process in which the no. 5 hydrogen of the orbit {2, 5} and the no. 6 hydrogen of the orbit {3, 6} in the right stereoisogram of Fig. 11 are replaced by proligand A's under a chiral condition. Note that no. 2 and no. 5 (or no. 3 and no. 6) of the  $C'_s(/C_1)$ -orbit are enantiotopic to each other (Table 2). The resulting stereoisogram belongs to Type II, as shown in the left of Fig. 19. The process of converting **24** into **40** (or  $\overline{\mathbf{40}}$ ) can be regarded as an asymmetric (chiral) synthesis, the total feature of which is shown by the conversion from Type IV (Fig. 11 right) to Type II (Fig. 19 left). Note that the equality symbols along the C-axis of Type IV (Fig. 11 right) is converted into the double-headed arrows of Type II (Fig. 19 left).

It should be noted that the products **40** and  $\overline{\mathbf{40}}$  cannot be differentiated by the *C/A*-convention shown in Fig. 15, even though they are enantiomeric to each other. By adopting the mode of numbering shown in the top of Fig. 15, the promolecule **40** is named 1-p-4- $\bar{p}$ -2,6-di-A-prismane and its enantiomers  $\overline{\mathbf{40}}$  is named 1-p-4- $\bar{p}$ -3,5-di-A-prismane.

2. (Pro-*RS*-stereogenicity along the S-axis) At the same time, the four hydrogens are subdivided into two two-membered orbits, i.e., {2, 3} and {5, 6}, each of which governed by a coset representation  $C_{1\bar{\sigma}}(/C_1)$ . For the *RS*-permutation group  $C_{1\bar{\sigma}}$ , see Eq. 29. Hence, the two orbits {2, 3} and {5, 6} are *RS*-enantiotropic, so that the promolecule **24** is concluded to be pro-*RS*-stereogenic.

The pro-*RS*-stereogenic concerned with the two *RS*-enantiotropic orbits {2, 3} and {5, 6} can be confirmed by a process in which the no. 2 hydrogen of the orbit {2, 3} and the no. 5 hydrogen of the orbit {5, 6} in the right stereoisogram of Fig. 11 are replaced by proligand A's, because 2 and 3 of {2, 3} (or 5 and 6 of {5, 6}) are already inequivalent geometrically (or energetically). In other words,

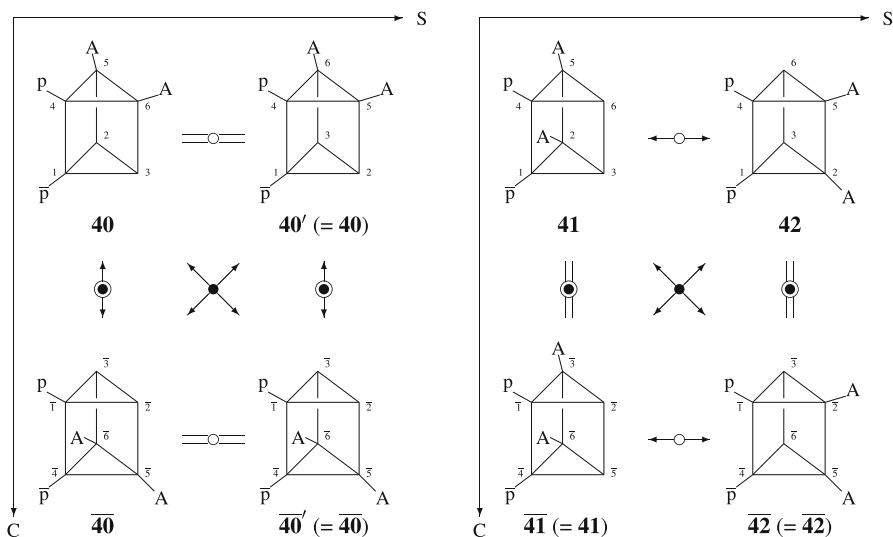


**Fig. 19** Stereoisograms of Type II (left) and Type V (right) for prismane derivatives with  $H_2A_2p\bar{p}$ , which are derived from the stereoisogram of Type IV for  $H_4p\bar{p}$  (the right of Fig. 11). The left diagram (Type II) is concerned with the products due to prochirality, while the right diagram (Type IV) is concerned with the products due to pro-*RS*-stereogenicity

no. 2 and no. 3 (or no. 5 and no. 6) of the  $C_{1\bar{\sigma}}(/C_1)$ -orbit are *RS*-diastereotopic to each other (Table 2). The resulting stereoisogram belongs to Type V, as shown in the right of Fig. 19. The process of converting an achiral promolecule **24** into an achiral promolecule **41** (or **42**) can be regarded as a usual reaction, the total feature of which is shown by the conversion from Type IV (Fig. 11 right) to Type V (Fig. 19 right). Note that the equality symbols along the *S*-axis of Type IV (Fig. 11 right) is converted into the double-headed arrows of Type V (Fig. 19 right).

According to the *C/A*-convention shown in Fig. 15, the product **41** is named (*a*)-1-*p*-4- $\bar{p}$ -2,3-di-*A*-prismane and the other product **42** is named (*c*)-1-*p*-4- $\bar{p}$ -2,3-di-*A*-prismane. They are *RS*-diastereomeric to each other, as differentiated by the *C/A*-convention, where the lowercase letters *c* and *a* are used because of achirality.

- (Prosclerality along the diagonal directions) Moreover, the four hydrogens are otherwise subdivided into two two-membered orbits, i.e., {2, 6} and {3, 5}, each of which governed by a coset representation  $C_2(/C_1)$ . For the ligand-reflection group  $C_2$ , see Eq. 27. Hence, the two orbits {2, 6} and {3, 5} are enantiocercal, so that the promolecule **24** is concluded to be proscleral. In other words, no. 2 and no. 6 (or no. 3 and no. 5) of the  $C_2(/C_1)$ -orbit are holantitopic to each other (Table 2). The prosclerality in a Type IV stereoisogram cannot be confirmed by such processes as described above for prochirality and pro-*RS*-stereogenicity. The process from asclerality to sclerality (i.e., the process due to prosclerality) already appear in the conversions of Fig. 11 (right) to Fig. 19 (left and right), where the



equality symbols along the diagonal directions in Fig. 11 (right) are converted into the double-headed arrows in Fig. 19 (left and right).

The stereoisogram approach is capable of integrating the three cases described above into a more sophisticated rationalization. The four H's of **24** constructs an orbit governed by a coset representation  $C_{1\sigma\hat{\sigma}2}/(C_1)$ , which is represented to be a symbolic coset representation  $G_{IV}/(H_{III})$  and characterized by a CR index  $\begin{bmatrix} a, a, a \\ -, -, - \end{bmatrix}$ . For the *RS*-stereoisomeric group  $C_{1\sigma\hat{\sigma}2}$ , see Eq. 31. The CR index indicates that the four-membered orbit governed by  $C_{1\sigma\hat{\sigma}2}/(C_1)$  is enantiospheric, *RS*-enantiotropic, and enantiocercal, so as to exhibit prochirality, pro-*RS*-stereogenicity, and prosclerality.

## 5 Conclusions

The stereoisogram approach developed by Fujita [10, 12] has been applied to discuss geometric prochirality an extended pseudoasymmetry by using prismane derivatives. By starting from the point group  $D_{3h}$  of order 12, the corresponding *RS*-stereoisomeric group of order 24 is generated for the purpose of discussing a prismane skeleton. In accord with a general proof [19], the existence of five types of stereoisograms (Types I–V) for prismane derivatives has been demonstrated by selecting illustrative examples from prismane derivatives with one achiral or chiral substituent, with two achiral substituents, with a pair of substituents enantiomeric in isolation, as well as with two chiral substituents of the same kind. After the proposal of a *C/A*-convention for characterizing absolute configurations, three intermolecular attributes (chirality, *RS*-stereogenicity, and sclerality) have been discussed by putting emphasis on the independence between chirality and *RS*-stereogenicity, extended aspects of pseudoasymmetry, and the assignability of *A/C*-descriptors. According to a general consideration proposed by us [20], three intramolecular attributes (prochirality, pro-*RS*-stereogenicity, and prosclerality) have been discussed on the basis of such attributive terms as sphericities, *RS*-tropicities, and cercalities, where illustrative examples are selected from prismane derivatives. In particular, special emphasis is laid on geometric prochirality appearing in stereoisograms of Type V, pro-*RS*-stereogenicity appearing in stereoisograms of Type II, prosclerality appearing in stereoisograms of Type I, superposition of prochirality and pro-*RS*-stereogenicity in stereoisograms of Type IV, as well as concurrent appearance of these attributes in stereoisograms of Type IV.

## References

1. N.G. Connelly, T. Damhus, R.M. Hartshorn, A.T. Hutton, *Nomenclature of Inorganic Chemistry. IUPAC Recommendations 2005* (The Royal Society of Chemistry, Cambridge, 2005)
2. E.L. Eliel, S.H. Wilen, *Stereochemistry of Organic Compounds* (Wiley, New York, 1994)
3. E. Fischer, *Aus Meinem Leben* (Springer, Berlin, 1922)
4. E. Fischer, Ber. Dtsch. Chem. Ges. **24**, 1836–1845 (1891)
5. E. Fischer, Ber. Dtsch. Chem. Ges. **24**, 2683–2687 (1891)
6. S. Fujita, Prochirality and Pro-*RS*-Stereogenicity. Stereoisogram Approach Free from the Conventional “Prochirality” and “Prostereogenicity”, in Carbon Bonding and Structures. Advances in Physics and Chemistry, ed. by M.V. Putz, Vol. 5 of Carbon Materials: Chemistry and Physics, Chapter 10. (Springer, Dordrecht, 2011), pp. 227–271

7. S. Fujita, *Tetrahedron* **47**, 31–46 (1991)
8. S. Fujita, *J. Chem. Inf. Comput. Sci.* **32**, 354–363 (1992)
9. S. Fujita, *Polyhedron* **12**, 95–110 (1993)
10. S. Fujita, *J. Org. Chem.* **69**, 3158–3165 (2004)
11. S. Fujita, *J. Math. Chem.* **35**, 265–287 (2004)
12. S. Fujita, *Tetrahedron* **60**, 11629–11638 (2004)
13. S. Fujita, *MATCH Commun. Math. Comput. Chem.* **52**, 3–18 (2004)
14. S. Fujita, *MATCH Commun. Math. Comput. Chem.* **52**, 3–18 (2004)
15. S. Fujita, *Memoirs of the faculty of engineering and design. Kyoto Inst Technol* **53**, 19–38 (2005)
16. S. Fujita, *J. Chem. Inf. Comput. Sci.* **44**, 1719–1726 (2004)
17. S. Fujita, *MATCH Commun. Math. Comput. Chem.* **53**, 147–159 (2005)
18. S. Fujita, *J. Math. Chem.* **47**, 145–166 (2010)
19. S. Fujita, *MATCH Commun. Math. Comput. Chem.* **54**, 39–52 (2005)
20. S. Fujita, *Tetrahedron* **62**, 691–705 (2006)
21. S. Fujita, *MATCH Commun. Math. Comput. Chem.* **61**, 39–70 (2009)
22. S. Fujita, *J. Comput. Aided Chem.* **10**, 76–95 (2009)
23. S. Fujita, *MATCH Commun. Math. Comput. Chem.* **61**, 11–38 (2009)
24. S. Fujita, *J. Comput. Aided Chem.* **10**, 16–29 (2009)
25. S. Fujita, *Tetrahedron* **65**, 1581–1592 (2009)
26. S. Fujita, *MATCH Commun. Math. Comput. Chem.* **63**, 3–24 (2010)
27. S. Fujita, *MATCH Commun. Math. Comput. Chem.* **63**, 25–66 (2010)
28. S. Fujita, *J. Math. Chem.* **49**, 95–162 (2011)
29. S. Fujita, *Symmetry and Combinatorial Enumeration in Chemistry* (Springer, Berlin, 1991)
30. S. Fujita, *Helv. Chim. Acta* **85**, 2440–2457 (2002)
31. S. Fujita, *J. Math. Chem.* **32**, 1–17 (2002)
32. S. Fujita, *Chem. Rec.* **2**, 164–176 (2002)
33. S. Fujita, *Bull. Chem. Soc. Jpn.* **75**, 1863–1883 (2002)
34. S. Fujita, *Bull. Chem. Soc. Jpn.* **63**, 315–327 (1990)
35. S. Fujita, *Bull. Chem. Soc. Jpn.* **63**, 1876–1883 (1990)
36. S. Fujita, *J. Math. Chem.* **33**, 113–143 (2003)
37. IUPAC Commission on Nomenclature of Organic Chemistry, *Pure Appl. Chem.* **71**, 513–529 (1999)
38. S. Fujita, *J. Am. Chem. Soc.* **112**, 3390–3397 (1990)
39. S. Fujita, *J. Org. Chem.* **67**, 6055–6063 (2002)
40. K.R. Hanson, *J. Am. Chem. Soc.* **88**, 2731–2742 (1966)
41. IUPAC Organic Chemistry Division, *Pure Appl. Chem.* **68**, 2193–2222 (1996)
42. J.A. Le Bel, *Bull. Soc. Chim. Fr. (2)* **22**, 337–347 (1874)
43. J.H. van't Hoff, *La Chimie Dans L'Espace* (P. M. Bazendijk, Rotterdam, 1875)
44. J.H. van't Hoff, *Die Lagerung der Atome im Raume, (German Translation by F. Herrmann)* (Friedrich Vieweg und Sohn, Braunschweig, 1877)